



# PAPAGEI: OPEN FOUNDATION MODELS FOR OPTICAL PHYSIOLOGICAL SIGNALS

Arvind Pillai<sup>2\*</sup>, Dimitris Spathis<sup>1,3</sup>, Fahim Kawsar<sup>1,4</sup>, Mohammad Malekzadeh<sup>1</sup>

<sup>1</sup>Nokia Bell Labs, UK, <sup>2</sup>Dartmouth College, USA,

<sup>3</sup>University of Cambridge, UK, <sup>4</sup>University of Glasgow, UK

## ABSTRACT

Photoplethysmography (PPG) is the most widely used non-invasive technique for monitoring biosignals and cardiovascular health, with applications in both clinical settings and consumer health through wearable devices. Current machine learning models trained on PPG signals are mostly task-specific and lack generalizability. Previous works often used single-device datasets, did not explore out-of-domain generalization, or did not release their models, hindering reproducibility and further research. We introduce PAPAGEI, the first open foundation model for PPG signals. PAPAGEI is pre-trained on more than 57,000 hours of 20 million unlabeled segments of PPG signals using publicly available datasets exclusively. We evaluate against popular time-series foundation models and other benchmarks on 20 tasks of 10 diverse datasets spanning cardiovascular health, sleep disorders, pregnancy monitoring, and wellbeing assessment. Our architecture incorporates novel representation learning approaches that leverage differences in PPG signal morphology across individuals, enabling it to capture richer representations than traditional contrastive learning methods. Across 20 tasks, PAPAGEI improves classification and regression performance by an average of 6.3% and 2.9%, respectively, compared to other competitive time-series foundation models in at least 14 tasks. PAPAGEI is more data- and parameter-efficient than other foundation models or methods, as it outperforms 70x larger models. Beyond accuracy, we also investigate robustness against different skin tones, establishing a benchmark for bias evaluations of future models. Notably, PAPAGEI can be used out of the box as both a feature extractor and an encoder for other multimodal models, opening up new opportunities for multimodal health monitoring<sup>1</sup>.

## 1 INTRODUCTION

Photoplethysmography (PPG), a non-invasive optical sensing technique, is widely used for monitoring cardiovascular health and physiological signals in both clinical and consumer health applications (Charlton et al., 2023). From hospital pulse oximeters to smartwatches, PPG enables continuous health monitoring in various settings, bridging acute medical care and long-term health management. PPG signals can track a diverse range of health indicators, including cardiovascular health, blood pressure, mood, and sleep disorders (Sadad et al., 2022; Ave et al., 2015; Temko, 2017; Reiss et al., 2019; Liang et al., 2018a; Haddad et al., 2021; Schrupf et al., 2021).

Despite its widespread adoption, PPG presents significant challenges for machine learning (ML). These include high annotation costs due to the need for domain-specific expertise, especially in consumer health applications where recording conditions and subject heterogeneity vary greatly. PPG signals are also susceptible to noise and motion artifacts (Afandizadeh Zargari et al., 2023), and inherent variability due to factors like skin tone and body composition (Bent et al., 2020) complicates the development of generalizable ML models. Consequently, existing PPG datasets are often small,

\*Work done while at Nokia Bell Labs.

<sup>1</sup>Models, data pipelines, and code are available at: <https://github.com/nokia-bell-labs/papagei-foundation-model>

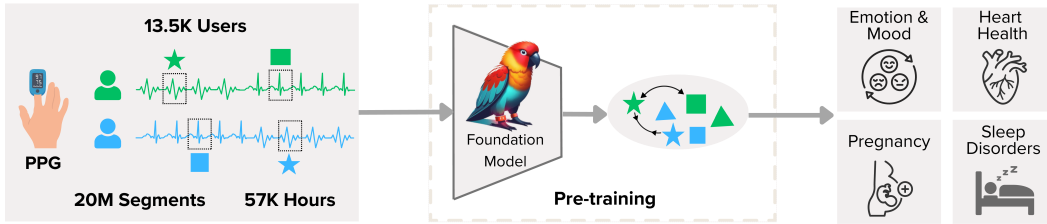


Figure 1: PAPAGEI Overview. We curate public datasets of diverse PPG signals, and train a foundation model leveraging a novel morphology-aware contrastive learning approach. To evaluate its effectiveness, we apply the embeddings generated by PAPAGEI to 20 tasks from 10 different datasets.

task-specific, and limited in their generalizability, posing a major obstacle to the development of robust and widely applicable models that could fully leverage the potential of this technology.

The PPG domain lacks general-purpose foundation models, unlike language and vision domains, with most work focused on single-dataset task-specific models. Although PPG signals detect vital signs like heart rate variability and blood oxygen saturation (Abbaspourazad et al., 2023; Charlton et al., 2023), the absence of generalizable pre-trained models limits progress. While there are difficulties in obtaining large-scale, high-quality datasets, recent increases in heterogeneous PPG data offer new opportunities (Johnson et al., 2016; Zhang et al., 2018; Lee et al., 2022). To address these challenges, we introduce **PAPAGEI**, a set of robust, pre-trained models capable of serving as a backbone for various PPG-related tasks, capturing rich PPG representations through large-scale pre-training.

Our key **contributions** are: **(1) Large-scale pre-training for PPG signals:** To our knowledge, PAPERAGEI is the first open foundation model pre-trained on PPG signals, using 57,000 hours of data from 20 million signals sourced entirely from public datasets. This establishes a new benchmark for large-scale model development in wearable and clinical health monitoring. **(2) PPG-aware self-supervised learning framework:** We introduce a novel self-supervised learning framework with a unique PPG signal morphology augmentation module. Our approach optimizes agreement between PPG signals with similar blood volume changes while learning signal quality and ratio around the dicrotic notch, a key PPG marker. **(3) Comprehensive evaluation across diverse out-of-domain health tasks:** We evaluate PAPERAGEI across 20 tasks, including cardiovascular health, sleep disorders, pregnancy monitoring, and overall well-being. Our results show that the model’s embeddings contain rich and predictive information applicable to various health conditions, outperforming existing benchmarks. **(4) Extensive robustness studies:** We conduct ablation studies to assess the impact of key components, including signal morphology augmentation, comparisons with established contrastive learning approaches, model size, data efficiency, and the effect of skin tone.

## 2 RELATED WORK

Self-supervised learning (SSL) has become a prominent paradigm for learning general representations from unlabeled datasets, with applications in physiological signal analysis including health, fitness, and brain signals (Tonekaboni et al., 2021; Zhang et al., 2022; Chen et al., 2021; Yèche et al., 2021; Spathis et al., 2021; Cheng et al., 2020; Kiyasseh et al., 2021; Sarkar & Etemad, 2020). Despite SSL’s popularity, there are no widely used pre-trained models for PPG signals. Recent studies have shown promise in this area, as (Abbaspourazad et al., 2023) demonstrated that embeddings from ECG and PPG signals can generalize across multiple health-related tasks using proprietary Apple Watch data. Similarly, (Yun et al., 2024) showed that embedding PPG signals can improve genetic discovery and risk prediction outcomes using the UK Biobank dataset. Other works (Weng et al., 2024; Ding et al., 2024; Zhou et al., 2024) explored PPG embeddings for various applications. However, these studies often used single-device datasets, did not explore out-of-domain generalization, or did not release their models, highlighting the need for openly available, pre-trained PPG foundation models.

While generic time-series foundation models like Chronos (Ansari et al., 2024) and Moment (Goswami et al., 2024) have gained popularity, they often lack significant physiological data representation. In contrast, our work takes a domain-specific approach, focusing exclusively on PPG

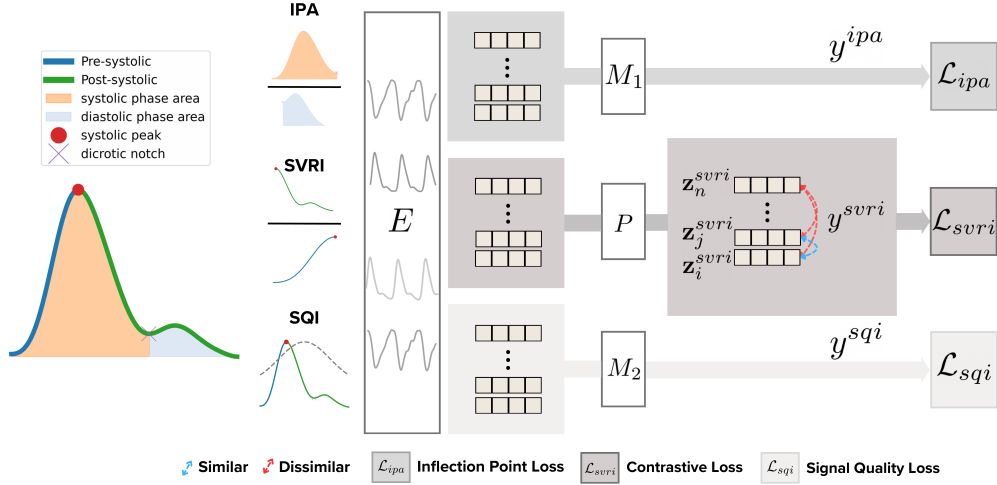


Figure 2: PAPAGEI-S Overview. Before training, for each PPG segment we compute the morphology metrics IPA, SVRI, and SQI, to be used as objectives (left). Next, we pass raw PPG signals through the encoder ( $E$ ), to extract embeddings (middle) and feed them into three heads (right): the projection head ( $P$ ) contrasts similar and dissimilar PPG signals based on sVRI, while two mixture-of-expert heads ( $M_1$  and  $M_2$ ) refine the embeddings by predicting IPA and SQI values, respectively.

signals. We argue that while knowledge from generic models may transfer to PPG tasks, performance is likely to be limited compared to a PPG-specific model. Similarly, transferring from other domain-specific models (e.g., ECG (McKeen et al., 2024; Song et al., 2024) or EEG (Yuan et al., 2024b)) to PPG is challenging due to differences in signal characteristics. Our specialized approach aims to capture the nuances and complexities specific to PPG signals, building on the increasing interest in modality-specific foundation models. See Appendix §F for more detailed discussions.

### 3 METHODS

Given a dataset  $\mathcal{D} = \{\mathbf{p}^1, \mathbf{p}^2, \dots, \mathbf{p}^S\}$  representing diverse PPG signals from  $S$  subjects, a PPG signal  $\mathbf{p}^s \in \mathbb{R}^n$  is defined as a time series that models the changes in light intensity due to arterial blood flow. To model granular changes in PPG signal of each subject  $s$ , we segment  $\mathbf{p}^s$  without overlap to obtain  $X^s = \{\mathbf{x}_1^s, \mathbf{x}_2^s, \dots, \mathbf{x}_N^s\}$ . Here, the number of segments  $N$  depends on the sampling frequency ( $f$ ) and the desired length of time window.

We use self-supervised learning to train PAPAGEI’s foundation model. We propose PAPAGEI-P, a *patient contrastive* approach that maximizes agreement between signals from the same subject. Importantly, we propose PAPAGEI-S, a *morphology-aware* self-supervised approach that maximizes agreement between signals with similar morphology. We present the details of both approaches.

#### 3.1 PARTICIPANT-AWARE OBJECTIVE

In PAPAGEI-P, we train a self-supervised learning model to maximize agreement between the latent embeddings of PPG signals from the same subject. While (Abbaspourzad et al., 2023) implements a similar strategy, they do not train or evaluate on public datasets.

**Training.** We define a positive pair as any two distinct segments from the same subject, denoted as  $\{(\mathbf{x}_i^s, \mathbf{x}_j^s) | i \neq j\}$ . Next, we apply a series of time series augmentations such as random cropping, adding Gaussian noise, time flipping, negation, and magnitude scaling (Tang et al., 2020). Each augmentation is applied with a predefined probability, determining its likelihood during training. Additionally, each augmentation includes hyper-parameters that control the intensity of the transformation. During training, the augmented versions of two randomly sampled positive pairs are passed through the encoder  $E$  and projection  $P$  to obtain embeddings denoted  $(\mathbf{z}_i^s, \mathbf{z}_j^s)$ . Given a batch of embeddings from  $N$  distinct subjects with positive pairs of the form  $(\mathbf{z}_i^s, \mathbf{z}_j^s)$ , the model optimizes the NT-Xent loss given by:  $\mathcal{L}_p = \frac{1}{2}(\ell_p(i, j) + \ell_p(j, i))$ , where

$\ell_p(i, j) = -\frac{1}{N} \sum_{i=1}^N \log \frac{\exp(\text{sim}(\mathbf{z}_i^s, \mathbf{z}_j^s)/\tau)}{\sum_{s \neq r} \exp(\text{sim}(\mathbf{z}_i^s, \mathbf{z}_j^r)/\tau)}$ . In contrast, vanilla SimCLR (Chen et al., 2020) uses positive pairs as augmented versions of randomly sampled PPG segments.

### 3.2 MORPHOLOGY-AWARE OBJECTIVE

In PAPAGEI-S, we leverage the PPG signal morphology to train a self-supervised learning model that maximizes agreement between similar physiological features of PPG signals across subjects.

**PPG Morphology.** Total peripheral resistance (TPR)—the force exerted by the body’s blood vessels on circulating blood—varies under certain medical conditions, such as hypertension and diabetes (Trammel & Sapa, 2020). Variations in TPR are reflected in PPG signals, presenting as distinct regions within the waveform (Figure 2, left). To capture these variations, we introduce a morphology augmentation module before training, which computes three key PPG metrics (Figure 2, left): (1) **stress-induced Vascular Response Index (sVRI)** (Lyu et al., 2015; Zhang et al., 2019): the ratio of mean PPG signal between post- to pre-systolic phases, (2) **Inflection Point Area ratio (IPA)** (Wang et al., 2009): the ratio of systolic to diastolic areas defined by the dicrotic notch, and (3) **Signal Quality index (SQI)**: skewness of the signal as an indicator of quality (Elgendi, 2016). We choose these metrics because they complement each other, with sVRI capturing amplitude variations, IPA reflecting signal width, and SQI addressing cases where IPA cannot be computed due to poor-quality signals lacking a dicrotic notch. We compute these metrics as follows:

$$sVRI(\mathbf{x}) = \frac{sys \sum_{i=sys}^n x_i}{(n - sys) \sum_{i=1}^{sys} x_i}, \quad IPA(\mathbf{x}) = \frac{\int_0^{\hat{n}} \mathbf{x} dn}{\int_{\hat{n}}^n \mathbf{x} dn}, \quad \text{and} \quad SQI(\mathbf{x}) = \frac{1}{W} \sum_w \frac{m_3}{m_2^{3/2}}, \quad (1)$$

where  $\mathbf{x} \in \mathbb{R}^N$  is the PPG segment, *sys* is the systolic peak, *n* is the length of time series, and  $\hat{n}$  is the dicrotic notch. For *SQI*, we divide  $\mathbf{x}$  into 5 second windows (*w*; total windows *W*) and compute the skewness  $m_i = \frac{1}{5 \times f} \sum_{j=1}^{5 \times f} (x[j] - \mu_x[j])^i$ , which gives the best signal quality discrimination (Elgendi, 2016).

**Training.** Before training, the morphology augmentation module takes an augmented (only Gaussian noise and cropping) input time series  $\mathbf{x}$  and outputs  $y = \{y^{svri}, y^{ipa}, y^{sqi}\} \in \mathbb{R}^3$  (Figure 2 middle). Next, we discretize  $y^{svri}$  into a predefined set of  $n = 8$  bins to denote positive pairs, where  $y^{svri} \in \{0, 1, \dots, n\}$ . We define positive pairs based on the sVRI labels as  $\{(\mathbf{x}_i, \mathbf{x}_j) | y_i^{svri} = y_j^{svri}, i \neq j\}$ . Note that positive pairs are not defined based on subjects.

Given a batch of *N* PPG signals and their morphology, we optimize three heads. First, we extract the embeddings  $Z = \{\mathbf{z}_1, \mathbf{z}_2, \dots, \mathbf{z}_N\}$  from the projection *P* (Figure 2 right middle), and compute the contrastive loss for sVRI (equation 2). Next, we use the embeddings  $H = \{\mathbf{h}_1, \mathbf{h}_2, \dots, \mathbf{h}_N\}$  to predict the IPA ( $\hat{y}^{ipa} \in \mathbb{R}^N$ ) and SQI ( $\hat{y}^{sqi} \in \mathbb{R}^N$ ) using the mixture of expert (MoE) heads  $M_1$  and  $M_2$ . Each MoE head is composed of three fully connected neural networks (FCNNs), with the head’s output calculated as a weighted sum of the FCNNs, using softmax to determine the weights. These heads are optimized using the mean absolute error (equation 3). The morphology indices encapsulate various PPG characteristics. Our rationale for utilizing MoE is that each expert can specialize in learning distinct properties that contribute to the overall index. Finally, the overall PAPAGEI-S training objective is given in equation 4.

$$\ell_s(i, j) = -\frac{1}{N} \sum_{i=1}^N \log \frac{\exp(\text{sim}(\mathbf{z}_i, \mathbf{z}_j)/\tau)}{\sum_{k \neq j} \exp(\text{sim}(\mathbf{z}_i, \mathbf{z}_k)/\tau)} \quad (2)$$

$$\mathcal{L}_{svri} = \frac{1}{2} (\ell_s(i, j) + \ell_s(j, i)) \quad \mathcal{L}_{ipa} = \frac{1}{N} \sum_{i=1}^N |y_i^{ipa} - \hat{y}_i^{ipa}| \quad \mathcal{L}_{sqi} = \frac{1}{N} \sum_{i=1}^N |y_i^{sqi} - \hat{y}_i^{sqi}| \quad (3)$$

$$\mathcal{L}_s = \alpha \mathcal{L}_{svri} + (1 - \alpha) (\mathcal{L}_{ipa} + \mathcal{L}_{sqi}), \text{ where } \alpha \in [0, 1] \quad (4)$$

## 4 EXPERIMENTS

### 4.1 PRE-TRAINING

**Datasets.** We curate three large public datasets to pre-train PAPAGEI (as shown in Table 1). The first dataset is VitalDB (Lee et al., 2022), which includes PPG signals collected during surgery from the finger using a patient monitor ( $f=500\text{Hz}$ ). The second dataset is the MIMIC-III waveform database matched subset (Johnson et al., 2016), where finger-tip PPG data is collected from an ICU monitor ( $f=125\text{Hz}$ ). The third dataset comes from the Multi-Ethnic Study of Atherosclerosis (MESA) sleep sub-study (Zhang et al., 2018; Chen et al., 2015), which provides PPG data obtained through finger-tip polysomnography ( $f=256\text{Hz}$ ). In total, we have 13.5K subjects with 20M segments.

**Pre-processing.** To curate and harmonize the PPG signals across all datasets, we perform the following steps based on established practices: (1) Apply a 4th-order Chebyshev bandpass filter with low and high pass cut-offs set at 0.5Hz and 12Hz, respectively (Lapitan et al., 2024; Liang et al., 2018c); (2) Segment the signal into 10-second windows (Orphanidou, 2018; Koteska et al., 2022); (3) Detect flatline segments and remove any segment where more than 25% of the data is flat (BioBSS Documentation, 2023); (4) Normalize the segments using Z-score (Abbaspourazad et al., 2023; Temko, 2017; Zhou et al., 2017); and (5) Resample the segments to 125Hz (the lowest sampling rate of our pre-training datasets, MIMIC-III).

**Implementation.** Recent work in PPG modeling has extensively used small-scale CNN architectures (Abbaspourazad et al., 2023; Ding et al., 2024). Building on that, we implement a ResNet-style (He et al., 2016) CNN encoder with 18 convolutional blocks, starting with a filter size of 32, which doubles every 4 blocks. The projection layer is a single FC layer, generating a 512-d embedding. In the PAPAGEI-S variant, the expert block ( $M_1$  &  $M_2$ ) uses three parallel FCNNs, each with two FC layers, resulting in a 128-d embedding. For augmentations, PAPAGEI-P uses cropping (0.50), negation (0.20), flipping (0.20), and scaling (0.40). PAPAGEI-S uses cropping (0.25) and Gaussian noise (0.25). PAPAGEI-S avoids augmentations that alter PPG’s morphology. We set  $\alpha = 0.6$  and train on eight V100 GPUs for 15,000 steps ( $\text{lr}=10^{-4}$ ), with PAPAGEI-P and PAPAGEI-S having 5M and 5.7M parameters, respectively (we study scaling in Section 5.2).

### 4.2 DOWNSTREAM TASKS

To evaluate the effectiveness of PAPAGEI, we benchmark it against a diverse set of datasets, tasks, and baselines, chosen for their large size and clinical relevance (where applicable)<sup>2</sup>. A brief de-

Table 1: Pre-training datasets.

Dataset	#Subjects	#Segments	Hours
VitalDB	5,866	6,248,100	17,355
MIMIC-III	5,596	7,196,401	19,990
MESA	2,055	7,306,705	20,296
Total	13,517	20,751,206	57,641

Table 2: The task evaluation benchmark of PAPAGEI. Datasets in grey are unseen during training (out-of-domain). The rest are used for pre-training (held-out test-sets and labels). Task types in brackets are B: binary, R: regression, M-#classes: multiclass classification.

#ID	Dataset	Task	#Subj.(#Samp.)
T1	VitalDB (Lee et al., 2022)	ICU admission (B)	5866
T2		Operation Type (M-9)	5866
T3	MIMIC-III (Moody et al., 2020)	Mortality (B)	5596
T4	MESA (Zhang et al., 2018)	Smoker (B)	2055
T5		AHI > 3% Oxygen Desat. (R)	2055
T6		AHI > 4% Oxygen Desat. (R)	2055
T7	nuMom2B (Facco et al., 2015)	Pregnancy stage (B)	3163 (5337)
T8		Gestation Age (R)	3163 (5337)
T9	VV (Skin Tone) (Toye, 2023)	Systolic BP* (R)	231
T10		Diastolic BP* (R)	231
T11	PPG-BP (Liang et al., 2018a)	Systolic BP (R)	219
T12		Diastolic BP (R)	219
T13		Average Heart Rate (R)	219
T14		Hypertension (B)	219
T15	SDB (Garde et al., 2014)	Sleep Disordered Breathing (B)	146
T16	ECSMP (Gao et al., 2021)	Mood Disturbance (B)	89
T17	WESAD (Schmidt et al., 2018)	Valence (B)	15 (4497)
T18		Arousal (B)	15 (4497)
T19	PPG-DaLiA (Reiss et al., 2019)	Heart Rate (R)	15 (64697)
T20		Activity (M-9)	15 (64697)

<sup>2</sup>[https://peterhcharlton.github.io/post/ppg\\_datasets/](https://peterhcharlton.github.io/post/ppg_datasets/)

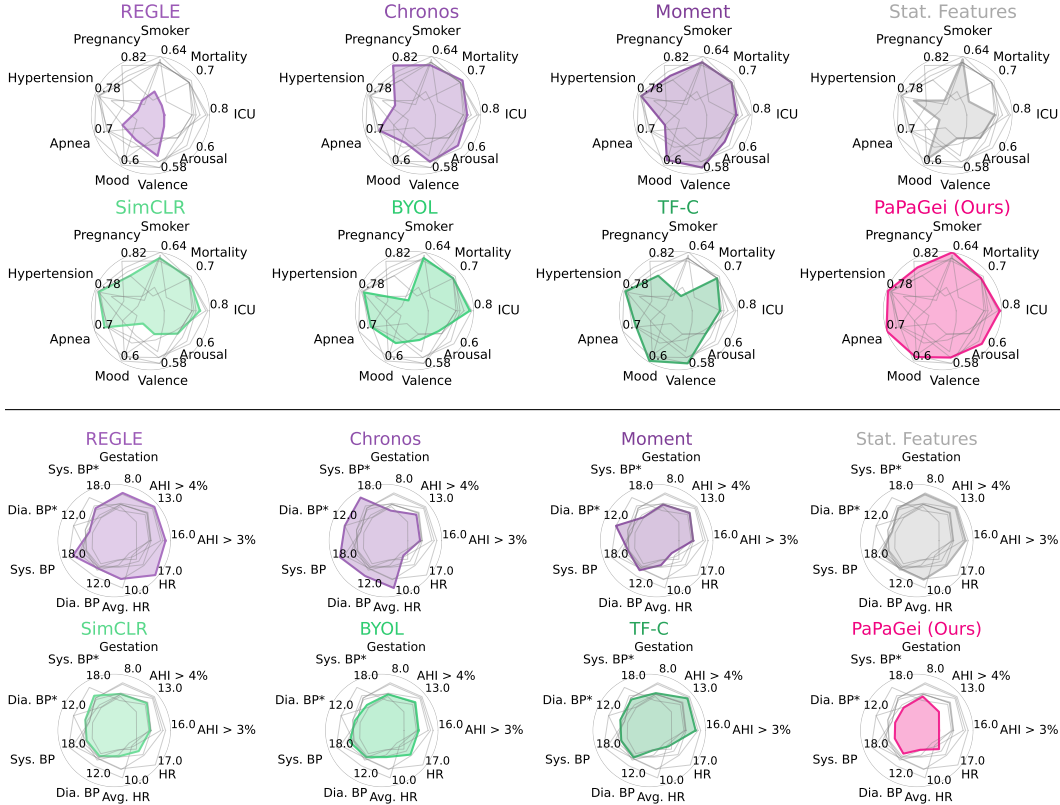


Figure 3: Radar charts of downstream tasks. (Top) *Classification* performance in **AUROC (larger area is better)**. (Bottom) *Regression* performance in **MAE (smaller area is better)**. Pre-trained models in purple: REGLE, Chronos, & Moment. Statistical feature baseline in gray. SSL methods in green: SimCLR, BYOL, & TF-C. PAPAAGEI (ours), in pink. Details are in Tables 3 & 4.

scription of the tasks with their corresponding #ID is provided in Table 2, with further details in Appendix B.

Identifying patient risk factors is crucial for hospitals to allocate resources effectively. To address this, we evaluate several indicators, including ICU admission (T1), type of operation (T2), mortality (T3), and smoking status (T4). For sleep apnea diagnosis, the American Academy of Sleep Medicine (AASM) recommends using the Apnea/Hypopnea Index (AHI) with at least 3% or 4% oxygen desaturation as a key metric (Ruehland et al., 2009). Thus, we predict AHI at 3% and 4% desaturation thresholds (T5 & T6) and classify sleep-disordered breathing (T15). For pregnancy outcomes, changes in gestational age and pregnancy stage are linked to risks like hypertensive disorders and small-for-gestational-age delivery (Bouariu et al., 2022; Wu et al., 2020; Crump et al., 2023), enabling us to classify pregnancy stage (T7) and predict gestational age (T8). In cardiovascular health, we estimate systolic (T9 & T11) and diastolic (T10 & T12) blood pressure (BP) using two datasets. While PPG-BP (T11 & T12) provides high-frequency, short PPG signals, the VV dataset helps explore skin tone’s influence on BP estimation. We also assess hypertension classification (T14), average seated heart rate (T13), and continuous heart rate during activities (T19), along with activity classification (T20). In the emotion domain, we classify PPG signals into mood disturbance levels (T16), valence (T17), and arousal (T18).

### 4.3 BASELINES

We benchmark PAPAAGEI’s performance against competitive baselines. As open-source foundation models designed for physiological signals, PAPAAGEI is compared to recent time-series foundation models: **Chronos** (Ansari et al., 2024) and **MOMENT** (Goswami et al., 2024). To evaluate the merits of our SSL framework, we also compare PAPAAGEI with common SSL methods (trained from

Table 3: **Downstream comparison against pre-trained models.** The model size is denoted next to their names. 95% CIs are reported in square brackets and the best value is **bolded**.

	<b>REGLE</b> (0.07M) (Yun et al., 2024)	<b>Chronos</b> (200M) (Ansari et al., 2024)	<b>Moment</b> (385M) (Goswami et al., 2024)	<b>PAPAGEI-P</b> (5M)	<b>PAPAGEI-S</b> (5.7M)
<b>Classification - AUROC (<math>\uparrow</math>)</b>					
ICU Admission	0.57 [0.52-0.62]	0.73 [0.68-0.80]	0.72 [0.70-0.80]	0.73 [0.67-0.78]	<b>0.79</b> [0.75-0.82]
Mortality	0.55 [0.52-0.59]	<b>0.68</b> [0.65-0.71]	0.67 [0.63-0.71]	0.67 [0.63-0.71]	0.67 [0.63-0.70]
Smoker	0.54 [0.47-0.59]	0.62 [0.57-0.67]	0.62 [0.56-0.67]	<b>0.64</b> [0.58-0.69]	0.61 [0.56-0.66]
Pregnancy stage	0.64 [0.57-0.63]	<b>0.81</b> [0.79-0.82]	0.76 [0.74-0.78]	0.74 [0.72-0.76]	0.78 [0.75-0.80]
Hypertension	0.47 [0.34-0.58]	0.57 [0.43-0.71]	0.75 [0.64-0.85]	0.74 [0.55-0.90]	<b>0.77</b> [0.68-0.87]
Sleep Disordered Breathing	0.45 [0.30-0.61]	0.58 [0.35-0.82]	0.45 [0.23-0.66]	0.54 [0.23-0.66]	<b>0.70</b> [0.57-0.84]
Mood Disturbance	0.41 [0.16-0.66]	0.43 [0.21-0.68]	0.55 [0.33-0.78]	0.53 [0.27-0.78]	<b>0.56</b> [0.33-0.77]
Valence	0.55 [0.52-0.57]	0.56 [0.53-0.59]	<b>0.57</b> [0.54-0.59]	0.53 [0.51-0.56]	0.56 [0.54-0.59]
Arousal	0.51 [0.52-0.58]	0.57 [0.54-0.60]	0.56 [0.53-0.58]	<b>0.58</b> [0.55-0.61]	0.55 [0.52-0.57]
Average	0.52 $\pm$ 0.06	0.62 $\pm$ 0.10	0.63 $\pm$ 0.09	0.63 $\pm$ 0.08	<b>0.67 <math>\pm</math> 0.09</b>
<b>Regression - MAE (<math>\downarrow</math>)</b>					
Apnea/Hypopnea Index > 3%	15.54 [14.20-16.69]	14.06 [13.05-15.16]	14.23 [13.04-15.42]	13.85 [12.43-15.49]	<b>12.97</b> [11.87-14.05]
Apnea/Hypopnea Index > 4%	12.64 [11.47-13.78]	11.57 [10.51-12.72]	11.80 [10.79-12.93]	11.24 [9.71-12.87]	<b>10.56</b> [9.59-11.62]
Gestation Age	7.28 [7.16-7.39]	<b>5.69</b> [5.54-5.85]	6.24 [6.10-6.37]	6.40 [6.21-6.59]	6.05 [5.91-6.17]
Systolic BP (VV)	15.88 [13.67-18.36]	17.24 [14.57-20.13]	14.71 [12.38-17.29]	19.11 [16.26-22.23]	<b>14.65</b> [12.50-16.78]
Diastolic BP (VV)	8.65 [7.16-10.27]	10.53 [8.91-12.19]	10.53 [8.91-12.19]	10.87 [9.10-12.98]	<b>8.29</b> [6.61-10.22]
Systolic BP (PPG-BP)	16.32 [13.87-19.13]	16.91 [13.31-19.34]	14.50 [11.98-17.31]	<b>13.60</b> [10.65-16.51]	14.39 [12.53-16.45]
Diastolic BP (PPG-BP)	9.30 [7.94-10.87]	10.26 [8.13-12.57]	9.53 [8.28-10.96]	8.88 [7.33-10.76]	<b>8.71</b> [7.18-10.01]
Average HR	6.88 [5.81-8.12]	8.51 [7.05-10.07]	4.41 [3.48-5.48]	<b>3.47</b> [2.74-4.32]	4.00 [3.34-4.67]
HR	16.35 [16.20-16.50]	9.65 [9.50-9.79]	<b>8.82</b> [8.68-8.96]	10.92 [10.80-11.04]	11.53 [11.40-11.66]
Average	12.09 $\pm$ 3.83	11.60 $\pm$ 3.60	10.43 $\pm$ 3.46	10.92 $\pm$ 4.25	<b>10.12 <math>\pm</math> 3.47</b>

scratch) such as **SimCLR** (Chen et al., 2020), **BYOL** (Grill et al., 2020), and **TF-C** (Zhang et al., 2022). In addition, to assess model generalizability on PPG signals, we compare against **REGLE**, a model pre-trained on UK Biobank’s PPG signals (Yun et al., 2024). As a simple baseline, we employ a random forest trained on **statistical features** extracted from the PPG signal, including mean, median, maximum, minimum, and the 25th, 50th, and 75th percentiles (“Stat. Features”). This task-specific approach serves as a benchmark for comparison with more advanced techniques.

#### 4.4 LINEAR EVALUATION

Initially, we split the in-domain and out-of-domain datasets into training, validation, and test sets at 80/10/10 and 60/20/20 ratios. The splitting is performed at the subject level ensuring no overlap between individuals across the sets. The models are evaluated by extracting feature representations from resampled data (125Hz) and applying linear probing for each task. For binary classification tasks, we employ a logistic regression model, with performance measured by the AUROC score. For regression tasks, ridge regression is used, and performance is evaluated based on the mean absolute error (MAE). Multi-class classification tasks are trained using a random forest model, with accuracy as the evaluation metric. To ensure robustness, we compute 95% confidence intervals (CIs) through bootstrapping (500 sampling runs with replacement). More details are provided in the Appendix §A.

## 5 RESULTS

### 5.1 OVERALL PERFORMANCE

In general, from Figure 3, we observe that PAPAGEI is more accurate across many tasks indicated by the larger AUROC area and smaller MAE area. Table 3 presents a more detailed comparison between PAPAGEI and other pre-trained models. For classification tasks, PaPaGei-S achieves the highest average AUROC of 0.67, outperforming other models across several tasks, particularly in ICU Admission (0.79), Hypertension (0.77), and Sleep Disordered Breathing (0.70). In regression tasks, PaPaGei-S again demonstrates strong performance, achieving the lowest average MAE (10.12), particularly in tasks related to Apnea/Hypopnea Index and BP measurements. REGLE, a small model trained on a large PPG dataset, generally underperforms compared to other models, suggesting its compact size may limit learning complex patterns. Chronos, a much larger model, shows competitive performance, particularly in Pregnancy Stage and Gestation Age prediction. Moment, the largest model, shows strong performance across many tasks, often matching or slightly outperform-

Table 4: **Downstream comparison against baseline and other SSL methods.** The model size is denoted next to their names. 95% CIs are reported in square brackets and the best value is **bolded**.

	Stat. Features	SimCLR (5M) (Chen et al., 2020)	BYOL (12M) (Grill et al., 2020)	TF-C (9.7M) (Zhang et al., 2022)	PAPAGEI-P (5M)	PAPAGEI-S (5.7M)
<b>Classification - AUROC (<math>\uparrow</math>)</b>						
ICU Admission	0.71 [0.65-0.78]	0.75 [0.72-0.79]	0.78 [0.73-0.81]	0.71 [0.67-0.75]	0.73 [0.67-0.78]	<b>0.79</b> [0.75-0.82]
Mortality	0.57 [0.54-0.61]	0.67 [0.63-0.70]	0.67 [0.64-0.71]	0.67 [0.63-0.70]	0.67 [0.63-0.71]	0.67 [0.63-0.70]
Smoker	0.63 [0.58-0.67]	0.62 [0.57-0.68]	0.62 [0.57-0.68]	0.61 [0.56-0.67]	<b>0.64</b> [0.58-0.69]	0.61 [0.56-0.66]
Pregnancy stage	0.64 [0.62-0.67]	0.74 [0.72-0.75]	0.62 [0.57-0.68]	0.74 [0.72-0.76]	0.74 [0.72-0.76]	<b>0.78</b> [0.75-0.80]
Hypertension	0.66 [0.47-0.83]	0.75 [0.64-0.86]	0.74 [0.64-0.84]	0.76 [0.63-0.86]	0.74 [0.55-0.90]	<b>0.77</b> [0.68-0.87]
SDB	0.32 [0.14-0.55]	0.61 [0.46-0.76]	0.59 [0.42-0.74]	0.58 [0.44-0.73]	0.54 [0.23-0.66]	<b>0.70</b> [0.57-0.84]
Mood Disturbance	0.54 [0.31-0.77]	0.32 [0.12-0.55]	0.46 [0.21-0.71]	<b>0.59</b> [0.33-0.84]	0.53 [0.27-0.78]	0.56 [0.33-0.77]
Valence	0.52 [0.49-0.55]	0.52 [0.49-0.55]	0.53 [0.50-0.56]	<b>0.57</b> [0.54-0.59]	0.53 [0.51-0.56]	0.56 [0.54-0.59]
Arousal	0.55 [0.53-0.58]	0.55 [0.52-0.58]	0.54 [0.30-0.78]	0.55 [0.52-0.58]	<b>0.58</b> [0.55-0.61]	0.55 [0.52-0.57]
Average	0.57 $\pm$ 0.11	0.61 $\pm$ 0.13	0.62 $\pm$ 0.10	0.64 $\pm$ 0.07	0.63 $\pm$ 0.08	<b>0.67 <math>\pm</math> 0.09</b>
<b>Regression - MAE (<math>\downarrow</math>)</b>						
Apnea/Hypopnea Index > 3%	15.31 [13.63-17.14]	14.17 [13.04-15.38]	14.26 [13.10-15.57]	15.10 [13.84-16.40]	13.85 [12.43-15.49]	<b>12.97</b> [11.87-14.05]
Apnea/Hypopnea Index > 4%	12.52 [10.92-14.14]	11.76 [10.65-12.89]	11.88 [10.71-13.05]	12.41 [11.33-13.49]	11.24 [9.71-12.87]	<b>10.56</b> [9.59-11.62]
Gestation Age	7.15 [6.99-7.34]	6.28 [6.21-6.49]	6.24 [6.09-6.38]	6.35 [6.21-6.49]	6.40 [6.21-6.59]	<b>6.05</b> [5.91-6.17]
Systolic BP (VV)	15.76 [13.67-18.36]	16.18 [13.73-18.85]	15.01 [12.32-17.80]	15.70 [13.23-18.13]	19.11 [16.26-22.23]	<b>14.65</b> [12.50-16.78]
Diastolic BP (VV)	9.75 [7.16-11.27]	9.15 [7.65-10.65]	8.91 [7.48-10.43]	9.15 [7.65-10.65]	10.87 [9.10-12.98]	<b>8.29</b> [6.61-10.22]
Systolic BP (PPG-BP)	15.50 [11.68-20.25]	14.38 [11.80-16.88]	14.99 [13.03-17.38]	14.45 [12.20-17.00]	<b>13.60</b> [10.65-16.51]	14.39 [12.53-16.45]
Diastolic BP (PPG-BP)	9.35 [7.44-11.66]	9.01 [7.90-10.60]	9.16 [8.00-10.50]	9.20 [7.90-10.60]	8.88 [7.33-10.76]	<b>8.71</b> [7.18-10.01]
Average HR	7.01 [5.48-8.89]	4.65 [3.99-5.39]	4.78 [3.88-5.93]	3.58 [2.90-4.21]	<b>3.47</b> [2.74-4.32]	4.00 [3.34-4.67]
HR	13.07 [12.90-13.23]	11.59 [11.46-11.72]	12.80 [12.66-12.94]	<b>9.99</b> [9.86-10.12]	10.92 [10.80-11.04]	11.53 [11.40-11.66]
Average	11.60 $\pm$ 3.41	10.79 $\pm$ 3.63	10.89 $\pm$ 3.58	10.65 $\pm$ 3.88	10.92 $\pm$ 4.25	<b>10.12 <math>\pm</math> 3.47</b>

ing Chronos. Notably, while PaPaGei-P shows competitive results, PaPaGei-S consistently outperforms it, suggesting the signal morphology objectives offer advantages in predictive capability.

Table 4 presents a comparison against three SSL methods and a baseline model trained on statistical features. In classification tasks, PaPaGei-S again shows the highest average AUROC, outperforming all others. SimCLR, BYOL, and TF-C generally outperform the statistical feature baseline but fall short of PaPaGei-S’s performance. TF-C shows competitive results in some tasks, achieving the highest AUROC for Mood Disturbance and Valence. For regression tasks, PaPaGei-S again achieves the lowest average MAE. SimCLR, BYOL, and TF-C show mixed results, as each excels in different tasks. SimCLR comes second in estimating Avg HR, while BYOL does so in Systolic BP (VV). The statistical feature baseline generally underperforms compared to the advanced methods across most tasks. PaPaGei-P, while not consistently outperforming PaPaGei-S, shows strong results that are often competitive with or better than other contrastive learning methods. Overall, both PaPaGei variants offer robust performance across a wide range of tasks.

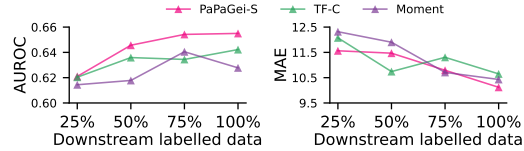


Figure 4: Downstream data-efficiency analysis. Results are averaged over all binary classification (left) and regression tasks (right). PAPAGEI-S performs better with increased label availability.

## 5.2 ABLATION STUDIES

**PAPAGEI-S component ablation.** We assess the impact of PAPAGEI-S components. Figure 5a & 5b show the full model consistently outperforms individual components in both mean and median metrics. On average, sVRI (0.64, 10.36) outperforms the combinations of sVRI + SQI (0.62, 10.81) and sVRI + IPA (0.64, 10.73), with SQI contributing the least to overall performance.

**Downstream data-efficiency analysis.** For limited-data scenarios, we assess the performance of downstream linear probing across varying levels of labeled data availability. We compare to the second best-performing baselines from Tables 3 & 4, namely TF-C and Moment. As shown in Figure 4, the classification performance of PAPAGEI-S steadily improves as more labeled data becomes available. While TF-C and Moment also show performance gains between 25% and 100% labeled data, their improvements are less consistent and smaller than PAPAGEI-S. In regression tasks, PAPAGEI-S achieves the lowest MAE at both 25% and 100% data availability, consistently reducing errors. At the middle breakpoints, the results are mixed with TF-C and Moment being competitive.

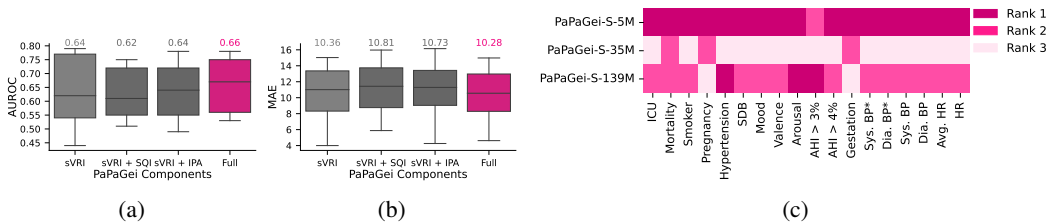


Figure 5: PAPA GEI-S component ablation study (a, b) and scaling analysis (c). (Left) The boxplot shows the performance of PAPA GEI-S components across all tasks. Despite the wide variation, the full model outperforms individual components. (Right) Heatmap ranks of PAPA GEI-S models with 5M, 35M, and 139M parameters (rank 1 denotes the best performance). Detailed results in Table 13.

**Model size and scaling analysis.** We evaluated whether larger model sizes improve performance by additionally training PAPA GEI-S-35M and PAPA GEI-S-139M with 35M and 139M parameters, respectively. Both models have the same number of layers, but the 35M model uses a 32 starting filter size, while the 139M model uses 64. As shown in 5c, the smallest model with 5M parameters performs best in all tasks except one, indicating that smaller models are better suited for PPG data.

Notably, the 139M model outperforms the 35M but still falls short of the 5M, suggesting that wider models may offer improved performance. Furthermore, the added complexity of the 139M model is advantageous for capturing decision boundaries in classification compared to the 35M model, which could be attributed to the classification-like objectives of contrastive learning. However, it struggles with regression tasks, which demand more precise outputs.

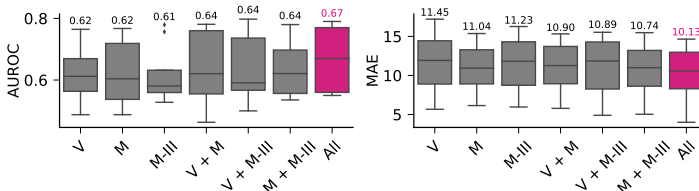


Figure 6: Ablation on pre-training datasets. Average performance across tasks for Binary classification (left) and regression (right) for models trained on different datasets: V (VitalDB), M (MESA), and M-III (MIMIC-III). The mean value is displayed above the plots.

**Pre-training data ablation.** We evaluated PAPA GEI-S using different combinations of pre-training data to determine if increasing the data volume enhances performance. Figure 6 demonstrates that performance on downstream tasks consistently improves as we incorporate additional upstream data, with optimal results achieved when utilizing all three datasets. Interestingly, in single datasets, MESA performs the best, despite having the fewest participants but the highest number of segments, echoing similar results in the language model domain (Dubey et al., 2024).

### 5.3 CASE STUDIES

To evaluate the downstream performance of PAPA GEI-S, we analyze the embedding distances among users within the sleep-disordered breathing dataset. We also investigate the model’s performance in predicting the Apnea-Hypopnea Index (AHI > 3%) and average Heart Rate. We analyze BP performance across different skin tones to evaluate robustness to different populations.

**Inter-participant embeddings.** Figure 7 shows the distribution of pair-wise embedding distances across participants (Kiyasseh et al., 2021). SimCLR and BYOL exhibit sharper peaks at lower distances, indicating that participants are more closely clustered within the embedding space. This could be interpreted as a mild form of mode collapse, where the model does not fully capture the individual

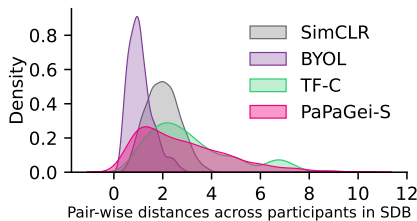


Figure 7: Pair-wise inter-participant embedding distances in sleep-disordered breathing.

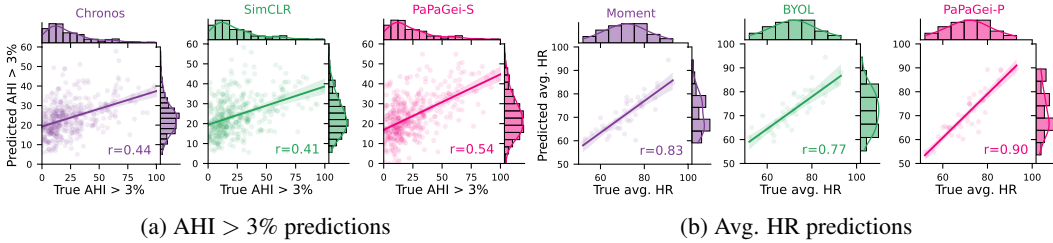


Figure 8: Regression plots with histograms for (a) Apnea/Hypopnea > 3% and (b) HR predictions. PAPAAGEI consistently matches the true label (scalar) distribution.

differences between participants. TF-C demonstrates a more balanced distribution, with both large and small peaks, suggesting it captures both similarities and some variation between participants. In contrast, PAPAAGEI-S provides the widest dispersion of embeddings, highlighting its ability to capture a broader range of features that may be valuable for distinguishing between participants’ medical conditions.

**Regression predictions.** In Figure 8, we observe that all models demonstrate positive correlations between true and predicted AHI. Compared to Chronos and SimCLR, PAPAAGEI-S shows superior regression performance ( $r=0.54$  vs.  $r=0.44$  and  $r=0.41$ ). This suggests that PAPAAGEI-S provides a more accurate prediction of AHI > 3% compared to Chronos and SimCLR, as it aligns more closely with the true AHI values. Moreover, PAPAAGEI-S demonstrates a higher correlation (0.90 vs. 0.77 and 0.83) for HR prediction. Examining the PAPAAGEI-P histograms reveals that the model effectively captures both tails of the distribution, reducing errors in the high and low heart rate ranges. In contrast, Moment and BYOL exhibit less consistent prediction distributions, leading to higher error rates.

**Skin tone analysis.** Understanding the impact of PPG models across skin tones is crucial for practical use (Bent et al., 2020; Sjoding et al., 2020). Therefore, we examine BP estimation performance across skin tones. As shown in Figure 9, PAPAAGEI-S achieves the best BP estimation across light tones. Across dark tones, we notice that BYOL and REGLE obtain the lowest MAE for Systolic BP and Diastolic BP, however, there are no significant differences across all models. While PAPAAGEI-S obtains the best overall performance, additional work is necessary to improve robustness on darker skin tones.

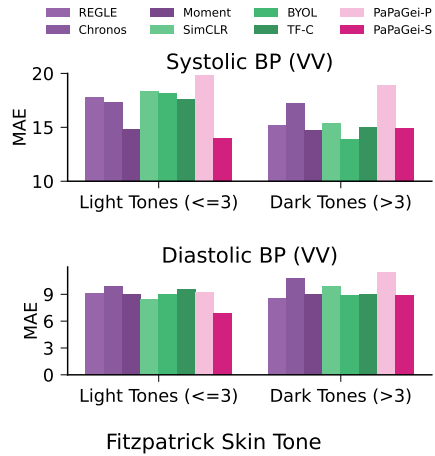


Figure 9: Skin tone analysis for Blood Pressure estimation (VV dataset). Figure 22 provides a breakdown across all skin tones.

## 6 CONCLUSION AND FUTURE WORK

Our results show that PAPAAGEI outperforms baselines in 14 tasks, with classification and regression improvements of 4.7%-6.3% and 2.9%-4.9%, respectively. PAPAAGEI-S excelled in cardiovascular tasks like BP, Hypertension, and HR, which can be attributed to the sVRI and IPA objectives, and PAPAAGEI-P outperformed baselines like Moment, excelling in tasks such as Smoking and Arousal. Ablation studies confirmed that the model with all three SSL objectives performs best, with sVRI highlighted as a key component and IPA and SQI providing positive knowledge transfer in multi-task setups. PAPAAGEI is both data- and size-efficient (5M), making it ideal for medical applications where large models (200M+) are impractical due to on-device limitations or data privacy concerns with cloud model inference. While combining PAPAAGEI-P and PAPAAGEI-S objectives into one model might seem intuitive, it is impractical because it would constrain positive pairs on both sVRI and the number of participants, resulting in too many unique labels with limited samples per label. Our case studies also showed that PAPAAGEI-S captured personal medical information due to well-

---

dispersed embeddings, compared to baselines. Future work should focus on diversifying training data, investigating sampling rate effects, and exploring multi-modal approaches or alternative architectures. In conclusion, PAPAGEI represents a significant advancement in foundation models for analyzing PPG signals in resource-constrained medical environments, with its open-source nature encouraging further research and development in healthcare applications.

## REPRODUCIBILITY STATEMENT

Models, data, and code will be made publicly available upon release, ensuring accessibility for future research. Our study exclusively utilizes publicly accessible datasets, which can be requested or downloaded from the respective study group websites, allowing others to easily obtain the data for their own analyses. In Section 4 and Appendix §B, we provide comprehensive descriptions of the datasets, ground-truth annotations, and data pre-processing methods used in our experiments, ensuring transparency in our data handling procedures. The code to run our model will be available with user-friendly examples. We have provided a detailed overview of the model architecture and its hyperparameters in Sections 3, 4.1, and Appendix §A. With these detailed resources, our work is designed to be reproducible, enabling future research to build upon our findings.

## ETHICS STATEMENT

Our research on PAPAGEI, utilizing publicly available PPG datasets, adheres to data privacy regulations and promotes transparency through open-source releases. We acknowledge potential biases in the training data and have evaluated performance across diverse datasets, particularly regarding skin tone variations. While PaPaGei offers significant potential for improving non-invasive health monitoring, we recognize the need to address potential misuse (Perez-Pozuelo et al., 2021). Examples of misuse could include unauthorized health monitoring, discriminatory practices in insurance or employment, unfair credit scoring, or exploiting personal health data for targeted marketing. We strongly advocate responsible use solely for beneficial healthcare applications. Our study followed established research ethics guidelines, and we declare no conflicts of interest. We encourage ongoing interdisciplinary dialogue to address potential risks and ensure responsible development and deployment of such technologies, recognizing the broader societal impacts of AI in healthcare. We remain committed to ethical AI advancement and welcome further discussion on the critical issues, including the development of governance frameworks to prevent misuse and protect data privacy.

## REFERENCES

- Salar Abbaspourazad, Oussama Elachqar, Andrew C Miller, Saba Emrani, Udhyakumar Nallasamy, and Ian Shapiro. Large-scale training of foundation models for wearable biosignals. *arXiv preprint arXiv:2312.05409*, 2023.
- Amir Hosein Afandizadeh Zargari, Seyed Amir Hossein Aqajari, Hadi Khodabandeh, Amir Rahmani, and Fadi Kurdahi. An accurate non-accelerometer-based ppg motion artifact removal technique using cyclegan. *ACM Transactions on Computing for Healthcare*, 4(1):1–14, 2023.
- Abdul Fatir Ansari, Lorenzo Stella, Caner Turkmen, Xiyuan Zhang, Pedro Mercado, Huibin Shen, Oleksandr Shchur, Syama Sundar Rangapuram, Sebastian Pineda Arango, Shubham Kapoor, et al. Chronos: Learning the language of time series. *arXiv preprint arXiv:2403.07815*, 2024.
- Arrozaq Ave, Hamdan Fauzan, S Rhandy Adhitya, and Hasballah Zakaria. Early detection of cardiovascular disease with photoplethysmogram (ppg) sensor. In *2015 international conference on electrical engineering and informatics (ICEEI)*, pp. 676–681. IEEE, 2015.
- Anastasiya Belyaeva, Justin Cosentino, Farhad Hormozdiari, Krish Eswaran, Shravya Shetty, Greg Corrado, Andrew Carroll, Cory Y McLean, and Nicholas A Furlotte. Multimodal llms for health grounded in individual-specific data. In *Workshop on Machine Learning for Multimodal Healthcare Data*, pp. 86–102. Springer, 2023.
- Brinnae Bent, Benjamin A Goldstein, Warren A Kibbe, and Jessilyn P Dunn. Investigating sources of inaccuracy in wearable optical heart rate sensors. *NPJ digital medicine*, 3(1):18, 2020.

- 
- BioBSS Documentation. Biobss: Biosignal processing toolbox. <https://biobss.readthedocs.io/en/latest/>, 2023. Accessed: 2024-09-10.
- Alexandra Bouariu, Anca Maria Panaitescu, and Kypros H Nicolaides. First trimester prediction of adverse pregnancy outcomes—identifying pregnancies at risk from as early as 11–13 weeks. *Medicina*, 58(3):332, 2022.
- Margaret M Bradley and Peter J Lang. Measuring emotion: the self-assessment manikin and the semantic differential. *Journal of behavior therapy and experimental psychiatry*, 25(1):49–59, 1994.
- Peter H Charlton, John Allen, Raquel Bailón, Stephanie Baker, Joachim A Behar, Fei Chen, Gari D Clifford, David A Clifton, Harry J Davies, Cheng Ding, et al. The 2023 wearable photoplethysmography roadmap. *Physiological measurement*, 44(11):111001, 2023.
- Hugh Chen, Scott M Lundberg, Gabriel Erion, Jerry H Kim, and Su-In Lee. Forecasting adverse surgical events using self-supervised transfer learning for physiological signals. *NPJ Digital Medicine*, 4(1):167, 2021.
- Ting Chen, Simon Kornblith, Mohammad Norouzi, and Geoffrey Hinton. A simple framework for contrastive learning of visual representations. *International conference on machine learning*, pp. 1597–1607, 2020.
- Xiaoli Chen, Rui Wang, Phyllis Zee, Pamela L Lutsey, Sogol Javaheri, Carmela Alcántara, Chandra L Jackson, Michelle A Williams, and Susan Redline. Racial/ethnic differences in sleep disturbances: the multi-ethnic study of atherosclerosis (mesa). *Sleep*, 38(6):877–888, 2015.
- Joseph Y Cheng, Hanlin Goh, Kaan Dogrusoz, Oncel Tuzel, and Erdrin Azemi. Subject-aware contrastive learning for biosignals. *arXiv preprint arXiv:2007.04871*, 2020.
- Casey Crump, Jan Sundquist, Mary Ann McLaughlin, Siobhan M Dolan, Usha Govindarajulu, Weiva Sieh, and Kristina Sundquist. Adverse pregnancy outcomes and long term risk of ischemic heart disease in mothers: national cohort and co-sibling study. *bmj*, 380, 2023.
- Cheng Ding, Zhicheng Guo, Zhaoliang Chen, Randall J Lee, Cynthia Rudin, and Xiao Hu. Siamquality: a convnet-based foundation model for photoplethysmography signals. *Physiological Measurement*, 45(8):085004, 2024.
- Abhimanyu Dubey, Abhinav Jauhri, Abhinav Pandey, Abhishek Kadian, Ahmad Al-Dahle, Aiesha Letman, Akhil Mathur, Alan Schelten, Amy Yang, Angela Fan, et al. The llama 3 herd of models. *arXiv preprint arXiv:2407.21783*, 2024.
- Mohamed Elgendi. Optimal signal quality index for photoplethysmogram signals. *Bioengineering*, 3(4):21, 2016.
- Francesca L Facco, Corette B Parker, Uma M Reddy, Robert M Silver, Judette M Louis, Robert C Basner, Judith H Chung, Frank P Schubert, Grace W Pien, Susan Redline, et al. Numom2b sleep-disordered breathing study: objectives and methods. *American journal of obstetrics and gynecology*, 212(4):542–e1, 2015.
- Mohammad Feli, Iman Azimi, Fatemeh Sarhaddi, Zahra Sharifi-Heris, Hannakaisa Niela-Vilen, Pasi Liljeberg, Anna Axelin, and Amir M Rahmani. Preterm birth risk stratification through longitudinal heart rate and hrv monitoring in daily life. 2024.
- Zhilin Gao, Xingran Cui, Wang Wan, Wenming Zheng, and Zhongze Gu. Ecsmp: A dataset on emotion, cognition, sleep, and multi-model physiological signals. *Data in Brief*, 39:107660, 2021.
- Ainara Garde, Parastoo Dehkordi, Walter Karlen, David Wensley, J Mark Ansermino, and Guy A Dumont. Development of a screening tool for sleep disordered breathing in children using the phone oximeter™. *PloS one*, 9(11):e112959, 2014.

- 
- Mononito Goswami, Konrad Szafer, Arjun Choudhry, Yifu Cai, Shuo Li, and Artur Dubrawski. Moment: A family of open time-series foundation models. *arXiv preprint arXiv:2402.03885*, 2024.
- Jean-Bastien Grill, Florian Strub, Florent Althé, Corentin Tallec, Pierre H Richemond, Elena Buchatskaya, Carl Doersch, Bernardo Avila Pires, Zhaohan Daniel Guo, Mohammad Gheshlaghi Azar, et al. Bootstrap your own latent—a new approach to self-supervised learning. *Advances in neural information processing systems*, 33:21271–21284, 2020.
- Nate Gruver, Marc Finzi, Shikai Qiu, and Andrew G Wilson. Large language models are zero-shot time series forecasters. *Advances in Neural Information Processing Systems*, 36, 2024.
- Serj Haddad, Assim Boukhayma, and Antonino Caizzone. Continuous ppg-based blood pressure monitoring using multi-linear regression. *IEEE journal of biomedical and health informatics*, 26(5):2096–2105, 2021.
- Kaiming He, Xiangyu Zhang, Shaoqing Ren, and Jian Sun. Deep residual learning for image recognition. In *Proceedings of the IEEE conference on computer vision and pattern recognition*, pp. 770–778, 2016.
- Kaiming He, Xinlei Chen, Saining Xie, Yanghao Li, Piotr Dollár, and Ross Girshick. Masked autoencoders are scalable vision learners. *Proceedings of the IEEE/CVF conference on computer vision and pattern recognition*, pp. 16000–16009, 2022.
- Alistair EW Johnson, Tom J Pollard, Lu Shen, Li-wei H Lehman, Mengling Feng, Mohammad Ghassemi, Benjamin Moody, Peter Szolovits, Leo Anthony Celi, and Roger G Mark. Mimic-iii, a freely accessible critical care database. *Scientific data*, 3(1):1–9, 2016.
- Dani Kiyasseh, Tingting Zhu, and David A Clifton. Clocs: Contrastive learning of cardiac signals across space, time, and patients. In *International Conference on Machine Learning*, pp. 5606–5615. PMLR, 2021.
- Bojana Koteska, Ana Madevska Bodanova, Hristina Mitrova, Marija Sidorenko, and Fedor Lehoccki. A deep learning approach to estimate spo2 from ppg signals. In *Proceedings of the 9th International Conference on Bioinformatics Research and Applications*, pp. 142–148, 2022.
- Denis G Lapitan, Dmitry A Rogatkin, Elizaveta A Molchanova, and Andrey P Tarasov. Estimation of phase distortions of the photoplethysmographic signal in digital iir filtering. *Scientific Reports*, 14(1):6546, 2024.
- Hyung-Chul Lee, Yoonsang Park, Soo Bin Yoon, Seong Mi Yang, Dongnyeok Park, and Chul-Woo Jung. Vitaldb, a high-fidelity multi-parameter vital signs database in surgical patients. *Scientific Data*, 9(1):279, 2022.
- Yongbo Liang, Zhencheng Chen, Guiyong Liu, and Mohamed Elgendi. A new, short-recorded photoplethysmogram dataset for blood pressure monitoring in china. *Scientific data*, 5(1):1–7, 2018a.
- Yongbo Liang, Zhencheng Chen, Rabab Ward, and Mohamed Elgendi. Hypertension assessment using photoplethysmography: a risk stratification approach. *Journal of clinical medicine*, 8(1):12, 2018b.
- Yongbo Liang, Mohamed Elgendi, Zhencheng Chen, and Rabab Ward. An optimal filter for short photoplethysmogram signals. *Scientific data*, 5(1):1–12, 2018c.
- Yongqiang Lyu, Xiaomin Luo, Jun Zhou, Chun Yu, Congcong Miao, Tong Wang, Yuanchun Shi, and Ken-ichi Kameyama. Measuring photoplethysmogram-based stress-induced vascular response index to assess cognitive load and stress. In *Proceedings of the 33rd annual ACM conference on human factors in computing systems*, pp. 857–866, 2015.
- Kaden McKeen, Laura Oliva, Sameer Masood, Augustin Toma, Barry Rubin, and Bo Wang. Ecg-fm: An open electrocardiogram foundation model. *arXiv preprint arXiv:2408.05178*, 2024.

- 
- Benjamin Moody, George Moody, Mauricio Villarroel, Gari D. Clifford, and Ikaro Silva. Mimi-iii waveform database matched subset (version 1.0), 2020. URL <https://doi.org/10.13026/c2294b>.
- Seungwhan Moon, Andrea Madotto, Zhaojiang Lin, Tushar Nagarajan, Matt Smith, Shashank Jain, Chun-Fu Yeh, Prakash Murugesan, Peyman Heidari, Yue Liu, et al. Anymal: An efficient and scalable any-modality augmented language model. *arXiv preprint arXiv:2309.16058*, 2023.
- Christina Orphanidou. Quality assessment for the photoplethysmogram (ppg). *Signal Quality Assessment in Physiological Monitoring: State of the Art and Practical Considerations*, pp. 41–63, 2018.
- Nisha I Parikh, Juan M Gonzalez, Cheryl AM Anderson, Suzanne E Judd, Kathryn M Rexrode, Mark A Hlatky, Erica P Gunderson, Jennifer J Stuart, Dhananjay Vaidya, American Heart Association Council on Epidemiology, Thrombosis Prevention; Council on Arteriosclerosis, Vascular Biology; Council on Cardiovascular, Stroke Nursing; and the Stroke Council. Adverse pregnancy outcomes and cardiovascular disease risk: unique opportunities for cardiovascular disease prevention in women: a scientific statement from the american heart association. *Circulation*, 143(18):e902–e916, 2021.
- Adam Paszke, Sam Gross, Francisco Massa, Adam Lerer, James Bradbury, Gregory Chanan, Trevor Killeen, Zeming Lin, Natalia Gimelshein, Luca Antiga, et al. Pytorch: An imperative style, high-performance deep learning library. *Advances in neural information processing systems*, 32, 2019.
- Ignacio Perez-Pozuelo, Dimitris Spathis, Jordan Gifford-Moore, Jessica Morley, and Josh Cowsls. Digital phenotyping and sensitive health data: Implications for data governance. *Journal of the American Medical Informatics Association*, 28(9):2002–2008, 2021.
- Attila Reiss, Ina Indlekofer, Philip Schmidt, and Kristof Van Laerhoven. Deep ppg: Large-scale heart rate estimation with convolutional neural networks. *Sensors*, 19(14):3079, 2019.
- Warren R Ruehland, Peter D Rochford, Fergal J O’Donoghue, Robert J Pierce, Parmjit Singh, and Andrew T Thornton. The new aasm criteria for scoring hypopneas: impact on the apnea hypopnea index. *sleep*, 32(2):150–157, 2009.
- Tariq Sadad, Syed Ahmad Chan Bukhari, Asim Munir, Anwar Ghani, Ahmed M El-Sherbeeney, and Hafiz Tayyab Rauf. Detection of cardiovascular disease based on ppg signals using machine learning with cloud computing. *Computational Intelligence and Neuroscience*, 2022(1):1672677, 2022.
- Pritam Sarkar and Ali Etemad. Self-supervised ecg representation learning for emotion recognition. *IEEE Transactions on Affective Computing*, 13(3):1541–1554, 2020.
- Philip Schmidt, Attila Reiss, Robert Duerichen, Claus Marberger, and Kristof Van Laerhoven. Introducing wesad, a multimodal dataset for wearable stress and affect detection. In *Proceedings of the 20th ACM international conference on multimodal interaction*, pp. 400–408, 2018.
- Fabian Schrumpf, Patrick Frenzel, Christoph Aust, Georg Osterhoff, and Mirco Fuchs. Assessment of deep learning based blood pressure prediction from ppg and rppg signals. In *Proceedings of the IEEE/CVF conference on computer vision and pattern recognition*, pp. 3820–3830, 2021.
- Michael W Sjoding, Robert P Dickson, Theodore J Iwashyna, Steven E Gay, and Thomas S Valley. Racial bias in pulse oximetry measurement. *New England Journal of Medicine*, 383(25):2477–2478, 2020.
- Junho Song, Jong-Hwan Jang, Byeong Tak Lee, DongGyun Hong, Joon-myung Kwon, and Yong-Yeon Jo. Foundation models for electrocardiograms. *arXiv preprint arXiv:2407.07110*, 2024.
- Dimitris Spathis and Fahim Kawsar. The first step is the hardest: Pitfalls of representing and tokenizing temporal data for large language models. *Journal of the American Medical Informatics Association*, 31(9):2151–2158, 2024.

- 
- Dimitris Spathis, Ignacio Perez-Pozuelo, Soren Brage, Nicholas J Wareham, and Cecilia Mascolo. Self-supervised transfer learning of physiological representations from free-living wearable data. In *Proceedings of the Conference on Health, Inference, and Learning*, pp. 69–78, 2021.
- Chi Ian Tang, Ignacio Perez-Pozuelo, Dimitris Spathis, and Cecilia Mascolo. Exploring contrastive learning in human activity recognition for healthcare. *arXiv preprint arXiv:2011.11542*, 2020.
- Andriy Temko. Accurate heart rate monitoring during physical exercises using ppg. *IEEE Transactions on Biomedical Engineering*, 64(9):2016–2024, 2017.
- Sana Tonekaboni, Danny Eytan, and Anna Goldenberg. Unsupervised representation learning for time series with temporal neighborhood coding. *arXiv preprint arXiv:2106.00750*, 2021.
- Pieter-Jan Toye. Vital videos: A dataset of videos with ppg and blood pressure ground truths. *arXiv preprint arXiv:2306.11891*, 2023.
- Jacob E Trammel and Amit Sapra. Physiology, systemic vascular resistance. 2020.
- L Wang, Emma Pickwell-MacPherson, YP Liang, and Yuan Ting Zhang. Noninvasive cardiac output estimation using a novel photoplethysmogram index. In *2009 annual international conference of the IEEE engineering in medicine and biology society*, pp. 1746–1749. IEEE, 2009.
- Wei-Hung Weng, Sebastien Baur, Mayank Daswani, Christina Chen, Lauren Harrell, Sujay Kakarmath, Mariam Jabara, Babak Behsaz, Cory Y McLean, Yossi Matias, et al. Predicting cardiovascular disease risk using photoplethysmography and deep learning. *PLOS Global Public Health*, 4(6):e0003204, 2024.
- Yuelin Wu, Sheng Wan, Shengyi Gu, Zhengqian Mou, Lingling Dong, Zhongcheng Luo, Jun Zhang, and Xiaolin Hua. Gestational weight gain and adverse pregnancy outcomes: a prospective cohort study. *BMJ open*, 10(9):e038187, 2020.
- Hugo Yèche, Gideon Dresdner, Francesco Locatello, Matthias Hüser, and Gunnar Rätsch. Neighborhood contrastive learning applied to online patient monitoring. In *International Conference on Machine Learning*, pp. 11964–11974. PMLR, 2021.
- Hang Yuan, Shing Chan, Andrew P Creagh, Catherine Tong, Aidan Acquah, David A Clifton, and Aiden Doherty. Self-supervised learning for human activity recognition using 700,000 person-days of wearable data. *NPJ digital medicine*, 7(1):91, 2024a.
- Zhizhang Yuan, Daoze Zhang, Junru Chen, Geifei Gu, and Yang Yang. Brant-2: Foundation model for brain signals. *arXiv preprint arXiv:2402.10251*, 2024b.
- Taedong Yun, Justin Cosentino, Babak Behsaz, Zachary R McCaw, Davin Hill, Robert Luben, Dongbing Lai, John Bates, Howard Yang, Tae-Hwi Schwantes-An, et al. Unsupervised representation learning on high-dimensional clinical data improves genomic discovery and prediction. *Nature Genetics*, pp. 1–10, 2024.
- Guo-Qiang Zhang, Licong Cui, Remo Mueller, Shiqiang Tao, Matthew Kim, Michael Rueschman, Sara Mariani, Daniel Mobley, and Susan Redline. The national sleep research resource: towards a sleep data commons. *Journal of the American Medical Informatics Association*, 25(10):1351–1358, 2018.
- Xiang Zhang, Ziyuan Zhao, Theodoros Tsiligkaridis, and Marinka Zitnik. Self-supervised contrastive pre-training for time series via time-frequency consistency. *Advances in Neural Information Processing Systems*, 35:3988–4003, 2022.
- Xiao Zhang, Yongqiang Lyu, Tong Qu, Pengfei Qiu, Xiaomin Luo, Jingyu Zhang, Shunjie Fan, and Yuanchun Shi. Photoplethysmogram-based cognitive load assessment using multi-feature fusion model. *ACM Transactions on Applied Perception (TAP)*, 16(4):1–17, 2019.
- Jianlong Zhou, Syed Z Arshad, Simon Luo, Kun Yu, Shlomo Berkovsky, and Fang Chen. Indexing cognitive load using blood volume pulse features. In *Proceedings of the 2017 CHI Conference Extended Abstracts on Human Factors in Computing Systems*, pp. 2269–2275, 2017.

---

Yuchen Zhou, Justin Cosentino, Taedong Yun, Mahantesh I Biradar, Jacqueline Shreibati, Dongbing Lai, Tae-Hwi Schwantes-An, Robert Luben, Zachary McCaw, Jorgen Engmann, et al. Utilizing multimodal ai to improve genetic analyses of cardiovascular traits. *medRxiv*, 2024.

# APPENDIX

## A TRAINING AND INFERENCE DETAILS

**Architecture & Pre-training.** The architecture of our ResNet 18-block encoder is described in Tables 5, 6, and 7. Each 1D convolution layer is configured with a kernel size of 3 and a stride of 2, while the max-pooling layer utilizes a kernel size of 3 with a stride of 1. We start with a filter size of 32, which doubles every 4 blocks to capture progressively more complex features. Dropout is applied with a probability of 0.5 to prevent overfitting. This backbone architecture is used across different methods in our experiments to ensure consistency and make for a fair comparison during evaluation. In PAPAGEI-S, we project the learned representations to a 512-dimensional embedding after the convolutional block (we investigated larger embedding sizes of 768 and 1024 and found no significant performance changes). This embedding is then passed through two Mixture of Experts (MoE) blocks, each containing three experts. Each expert block consists of two sequential linear layers, with sizes 256 and 1, which are used for IPA and SQI prediction tasks. It is noteworthy that both BYOL and TF-C require multiple encoders and different projection heads, resulting in variations in model sizes. For these methods, we use existing implementations available online<sup>3,4</sup>, but apply our encoder as the backbone to ensure consistency. Our models are pre-trained for 15,000 steps using the Adam optimizer, with a learning rate of  $10^{-4}$ . We use a batch size of 128 for training since after various trials we did not observe significant differences in performance with batch sizes of 64 and 256. Additionally, we did not perform an exhaustive evaluation of different augmentation settings but instead used transformations and values based on prior research (Abbaspourzad et al., 2023; Tang et al., 2020). For model training, we primarily used PyTorch (Paszke et al., 2019). The NTXentLoss implementation was sourced from the PyTorch Metric Learning package<sup>5</sup>.

Table 5: ResNet-style CNN encoder architecture used in PAPAGEI.

Layer	Output Shape
Conv1	[32, 32, 1250]
Batch Norm	[32, 32, 1250]
ReLU	[32, 32, 1250]
Basic Block Type 1	[32, 32, 1250]
(Basic Block Type 2) × 3	[32, 32, 313]
(Basic Block Type 2) × 4	[32, 64, 79]
(Basic Block Type 2) × 4	[32, 128, 20]
(Basic Block Type 2) × 4	[32, 256, 5]
(Basic Block Type 2) × 2	[32, 512, 3]
BatchNorm	[32, 512, 3]
ReLU	[32, 512, 3]
Linear	[32, 512]

Table 6: Basic Block Type 1

Layer
Conv1D
BatchNorm
ReLU
Dropout
Conv1D

Table 7: Basic Block Type 2

Layer
BatchNorm
ReLU
Dropout
Conv1D
BatchNorm
ReLU
Dropout
Conv1D
Maxpool

**Feature Extraction & Linear Evaluation** We extracted the projected embedding for linear evaluation. For Moment and Chronos, we extract the default embedding size, which is 1024 and 768, respectively. We use cross-validated grid search to identify the best parameters for our linear probes. The hyperparameters chosen for each model are as follows: (1) Logistic Regression: {'penalty': ['l1', 'l2'], 'C': [0.01, 0.1, 1, 10, 100], 'solver': ['lbfgs'], 'max\_iter': [100, 200]}. (2) Linear Regression: {'alpha': [0.1, 1.0, 10.0, 100.0], 'solver': ['auto', 'cholesky', 'sparse\_cg']}. (3) Random Forest: {'n\_estimators': [100, 200], 'max\_features': ['sqrt', 'log2'], 'max\_depth': [10, 20, 30], 'min\_samples\_split': [2, 5], 'min\_samples\_leaf': [1, 2]}

<sup>3</sup><https://github.com/chengding0713/SiamQuality>

<sup>4</sup><https://github.com/mims-harvard/TFC-pretraining>

<sup>5</sup><https://github.com/KevinMusgrave/pytorch-metric-learning>

## B DATASETS AND TASKS

Table 8: The task evaluation benchmark of PAPA<sub>GEI</sub>. Datasets highlighted in grey are unseen during training, thus, the corresponding tasks are out-of-domain. The rest were used for pre-training but their test sets and labels are held out. For task type, B/M/R refer to Binary classification, Multi-class classification (#classes), and Regression, respectively.

#ID	Dataset	SR (Hz)	Collected by	Task	Task Type	#Subjects (#Samples)
T1	VitalDB (Lee et al., 2022)	500	ICU monitor	ICU admission (Yes/No)	B	5866
T2				Operation Type	M (11)	5866
T3	MIMIC-III (Moody et al., 2020)	125	ICU Monitor	Mortality	B	5596
T4	MESA (Zhang et al., 2018)	256	Polysomnography finger	Smoker	B	2055
T5				AHI > 3% Oxygen Desat.	R	2055
T6				AHI > 4% Oxygen Desat.	R	2055
T7	nuMom2B (Facco et al., 2015)	75	Polysomnography finger	Pregnancy stage (early/late)	B	3163 (5337)
T8				Gestation Age	R	3163 (5337)
T9	VV (Skin Tone) (Toye, 2023)	60	Finger	Systolic BP	R	231
T10				Diastolic BP	R	231
T11	PPG-BP (Liang et al., 2018a)	1000	Finger Pulse Ox	Systolic BP	R	219
T12				Diastolic BP	R	219
T13				Average Heart Rate	R	219
T14				Hypertension	B	219
T15	SDB (Garde et al., 2014)	62.5	Finger Pulse Ox	Sleep Disordered Breathing	B	146
T16	ECSMP (Gao et al., 2021)	64	Wrist	Mood Disturbance	B	89
T17	WESAD (Schmidt et al., 2018)	64	Wrist	Valence	B	15 (4497)
T18				Arousal	B	15 (4497)
T19	PPG-DaLiA (Reiss et al., 2019)	64	Wrist	Heart Rate	R	15 (64697)
T20				Activity	M (9)	15 (64697)

**VitalDB.** The VitalDB dataset provides comprehensive monitoring of vital signs and physiological parameters from 6,388 surgical cases. This high-resolution dataset includes a wide range of intraoperative monitoring variables such as heart rate, blood pressure, oxygen saturation, and other critical physiological signals, collected at frequent intervals throughout surgery. The surgical operation belongs to one of the eleven categories: colorectal, biliary/pancreas, stomach, major resection, minor resection, breast, transplantation, thyroid, hepatic, vascular, and others. After the data cleaning process, we narrowed the dataset down to 5,866 subjects with complete and usable information. As depicted in Figure 10, we observe that the gender distribution is relatively balanced, with nearly equal representation of male and female patients. Additionally, the majority of the subjects fall within the age range of 50 to 70, with a significant proportion being around 60 years old. The ICU label corresponds to whether the person was admitted to the ICU or not.

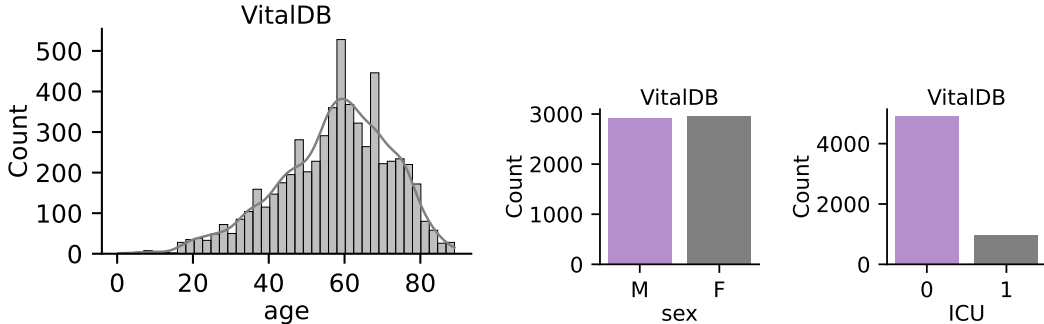


Figure 10: VitalDB dataset descriptive statistics.

**MIMIC-III.** In our analysis, we utilize the MIMIC-III waveform database matched subset, which comprises data from 10,282 ICU patients. From this dataset, we focus specifically on extracting photoplethysmogram (PPG) data, provided it is available for each patient. To ensure the quality of the data, we set a criterion of at least 1 minute of usable PPG signal that must be present. After performing a thorough data cleaning process, we end up with a cohort of 5,596 subjects with reliable PPG data. As illustrated in Figure 11, the dataset shows a gender imbalance, with a higher proportion of male patients compared to female patients. Additionally, the majority of subjects are aged 60 years or older, reflecting a typical ICU population that often includes elderly patients with critical health conditions.

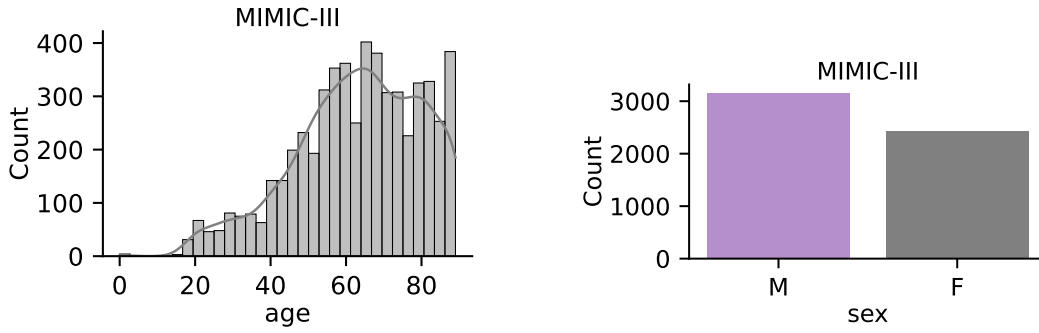


Figure 11: MIMIC-III dataset descriptive statistics.

**MESA.** The Multi-Ethnic Study of Atherosclerosis (MESA) sleep sub-study gathered data from 2,237 participants through overnight, unattended polysomnography to assess various sleep parameters. After the data cleaning process, we retained 2,055 subjects for analysis. As shown in Figure 12, the dataset shows a slightly larger proportion of female participants. The age distribution reveals that most subjects are between 60 and 80 years old, reflecting an older adult population, which is commonly studied concerning sleep disorders and cardiovascular risks.

In this study, we use the Apnea-Hypopnea Index (AHI) with at least 3% and 4% oxygen desaturation as the primary measure for diagnosing sleep apnea, as recommended by the American Academy of Sleep Medicine (AASM) (Ruehland et al., 2009). These thresholds indicate the severity of sleep apnea, with oxygen desaturation during apneas/hypopneas being a critical factor. We predict these AHI values directly in our regression models. Additionally, we classify participants with any history of smoking as smokers. This approach allows us to account for both current and former smokers, capturing a broader range of smoking-related health risks within our analysis.

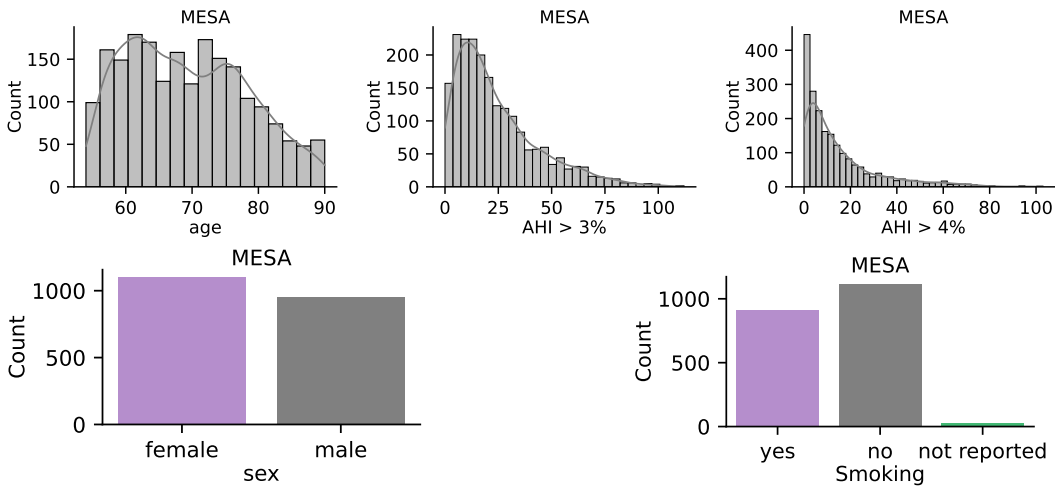


Figure 12: MESA dataset descriptive statistics.

**NuMoM2B.** Changes in gestational age and pregnancy stage are risk factors associated with adverse pregnancy outcomes such as hypertensive disorders and small-for-gestational-age delivery (Bouariu et al., 2022; Parikh et al., 2021; Wu et al., 2020; Crump et al., 2023). These diseases affect heart function that can be measured using the PPG sensor (Feli et al., 2024). The Nulliparous Pregnancy Outcomes Study: monitoring mothers-to-be (nuMoM2B) sub-study examines the relationship between adverse pregnancy outcomes and sleep disorders. In particular, an overnight polysomnograph that collects PPG data is administered to the women at their homes during 6-15 weeks (early) and 22-31 weeks (late) of pregnancy. Therefore, our tasks are to classify between early and late-stage pregnancy as well as predict the gestation age of the fetus. In Figure 13, we observe that maternal

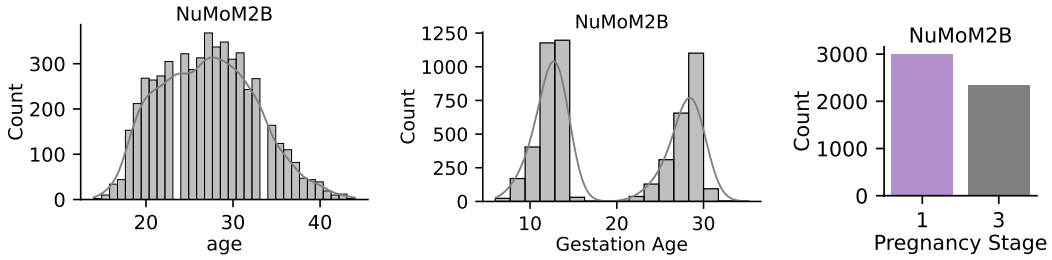


Figure 13: NuMoM2B dataset descriptive statistics.

age peaks around 28 years. The gestational age distribution is bimodal, which we use as a predictor in our regression task. For pregnancy stage, we classify visit 1 as early and visit 3 as late.

**VitalVideos (VV) (Skin Tone).** The Vital Videos study is an ongoing project that collects data on vital signs, videos, and blood pressure across a variety of conditions, including variations in lighting, background, and skin tone. For our analysis, we used data from two groups, totalling 231 subjects, from Europe and Sub-Saharan Africa. As shown in Figure 14, most subjects have a Fitzpatrick skin tone of 5 or 6, indicating darker skin. The dataset is primarily composed of female participants, with an age range between 40 and 60 years. Additionally, the majority of subjects had a systolic blood pressure of around 125 and a diastolic pressure of around 80, suggesting that most individuals in the study were relatively healthy.

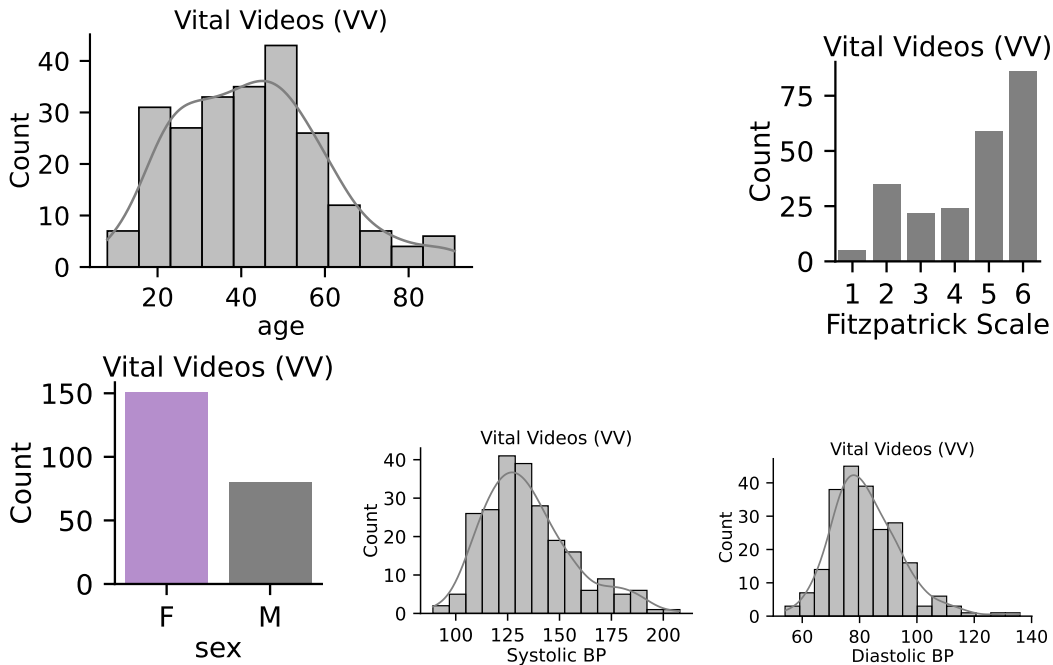


Figure 14: Vital Videos dataset descriptive statistics.

**PPG-BP.** The PPG-BP consists of short PPG recordings from 219 subjects collected at 1000Hz. For each subject, there are three 2.1s recordings. For our analysis, we zero pad them to 10s. In Figure 15, the age distribution shows that most subjects are between 40 and 80 years old, with fewer participants under 40. Furthermore, the majority of individuals have hypertension. In terms of gender, the dataset has slightly more females than males. The distribution of systolic blood pressure is centered around 120-140, indicating a population with normal to moderately elevated blood pressure, while diastolic blood pressure predominantly falls between 70 and 90. Lastly, the average heart rate for most subjects ranges between 70 and 90 beats per minute.

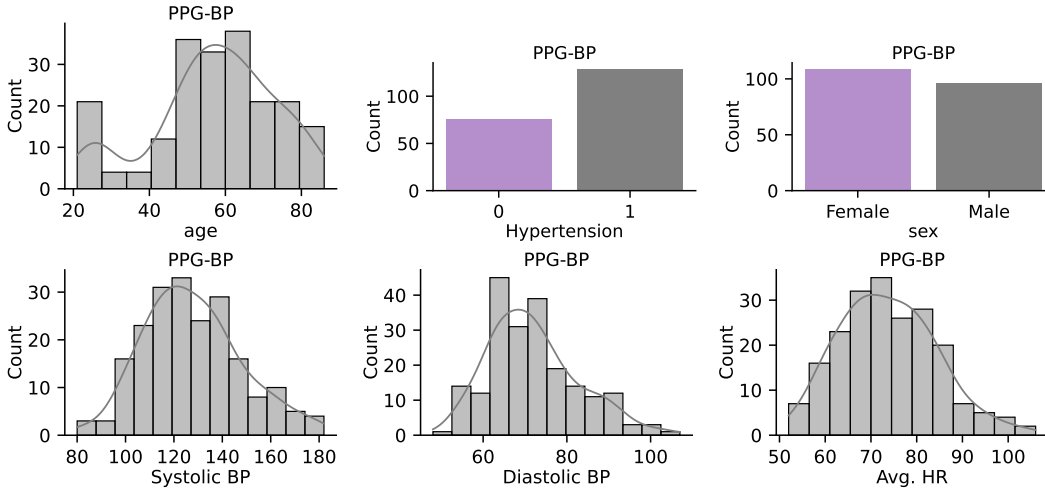


Figure 15: PPG-BP dataset descriptive statistics.

**SDB.** The sleep-disordered breathing dataset includes data from 146 children, collected through polysomnography with finger recordings lasting over three hours. Ground truth labels are provided as Apnea-Hypopnea Index (AHI) values, categorized into four levels: 0 (normal), 1 (mild, AHI between 5 and 15), 2 (moderate, AHI between 15 and 30), and 3 (severe, AHI over 30) as shown in Figure 16. For our classification task, we group AHI 0 as indicating no sleep breathing disorder, while AHI levels 1 through 3 are classified as the presence of a sleep breathing disorder.

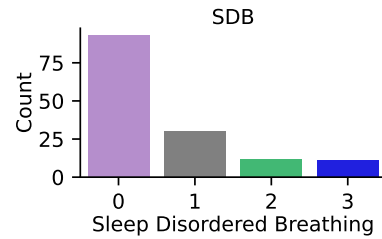


Figure 16: SDB dataset descriptive statistics.

**ECSMP.** The ECSMP dataset was gathered to study the relationship between emotion, cognition, and sleep in 89 subjects. As shown in Figure 17, the majority of the participants are young adult females, with an average age of around 25 years. Mood disturbances were measured using the Profile of Mood States (POMS) scale, which captures various aspects of emotional states. To classify participants into high versus low mood disturbance categories, we binarized the Total Mood Disturbance (TMD) values by using the median as the cutoff point.

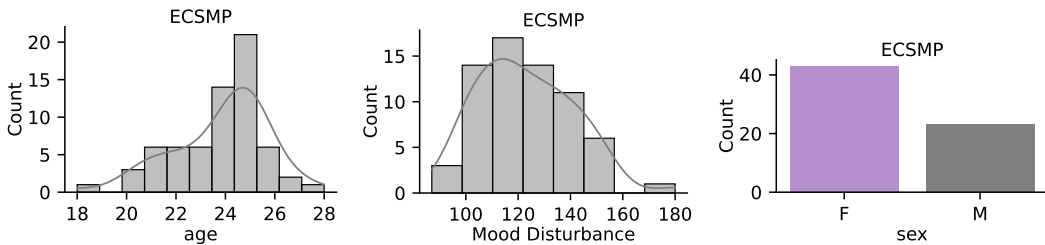


Figure 17: ECSMP dataset descriptive statistics.

**WESAD.** The wearable stress and affect detection dataset is a multi-modal dataset collected from 15 subjects using various sensor modalities. In this study, participants were exposed to videos designed to elicit different affective states, such as amusement, meditation, stress, and baseline conditions. Following each session, participants completed the Self-Assessment Manikins (SAM) questionnaire (Bradley & Lang, 1994), which provided the ground-truth values for valence and arousal. In our analysis, we binarized these values by categorizing valence and arousal as low (1) when less than 5 and high (0) otherwise. Then, we perform regression at the segment level. As shown in Figure 18, arousal levels are generally low, while valence tends to be high in most cases.

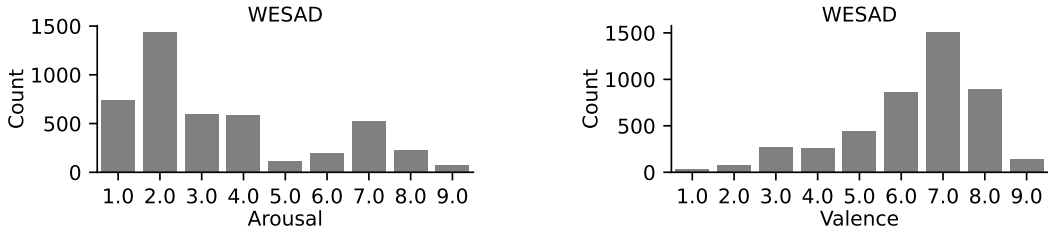


Figure 18: WESAD dataset descriptive statistics.

**PPG-DaLiA.** This dataset collects PPG signals from 15 subjects for heart rate estimation while performing various daily activities. These activities include sitting, ascending/descending stairs, table soccer, cycling, driving, lunch break, walking, and working. As a result, the dataset captures a wide range of heart rates, varying from 60 to 150 beats per minute, depending on the specific activity being performed.

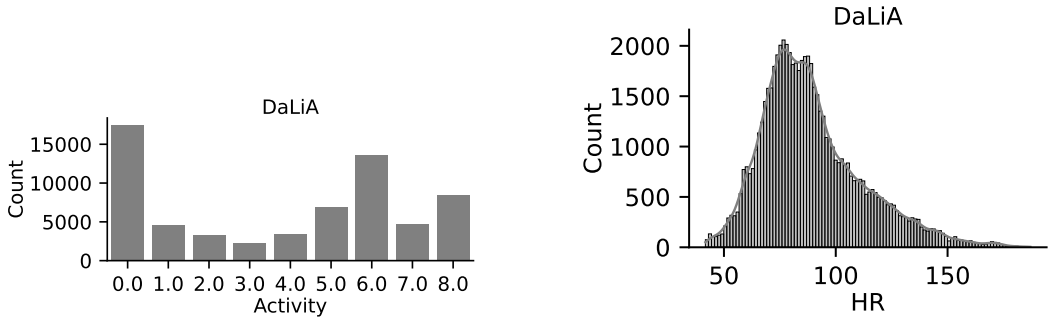


Figure 19: PPG-DaLiA dataset descriptive statistics.

---

## C REPRESENTATIVE SIGNALS FROM PRE-TRAINING DATASETS

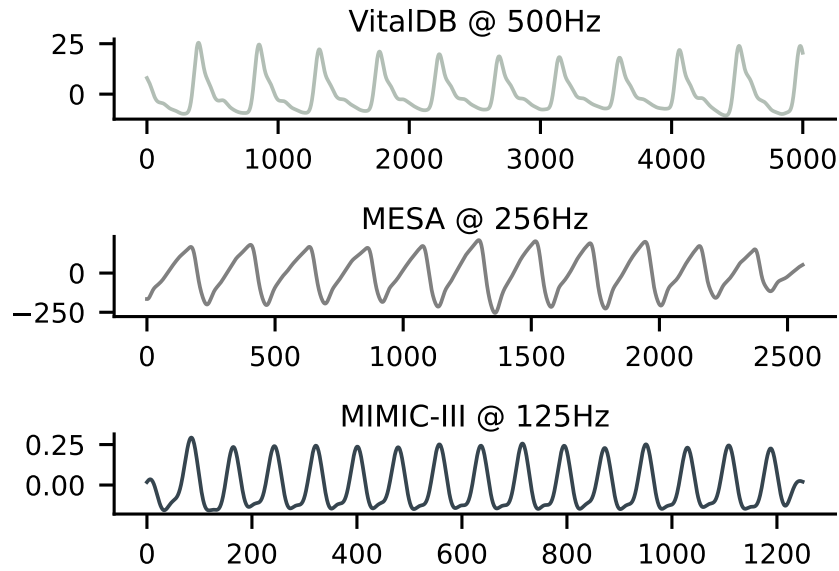


Figure 20: Representative 10-second *raw* PPG segments from VitalDB, MESA, and MIMIC-III. We observe that each signal’s amplitude (y-axis) and sampling rate differ.

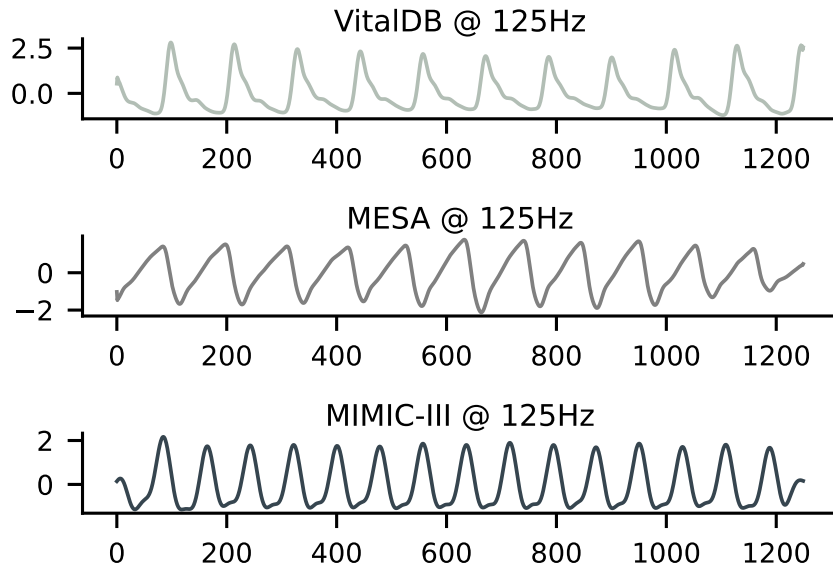


Figure 21: Normalized and resampled 10-second *pre-processed* PPG segments from VitalDB, MESA, and MIMIC-III. These signals represent the final form before being fed to our models. We observe that the signal characteristics across datasets are more consistent.

## D ADDITIONAL RESULTS

### D.1 MULTI-CLASS CLASSIFICATION

Table 9: **Multi-class classification comparison against pre-trained models.** The parameter size and reference are denoted next to their names. 95% CIs are reported in square brackets and the best value is **bolded**.

Classification - ACC ( $\uparrow$ )	REGLE (0.07M) (Yun et al., 2024)	Chronos (200M) (Ansari et al., 2024)	Moment (385M) (Goswami et al., 2024)	PAPAGEI-P (5M)	PAPAGEI-S (5.7M)
Operation Type	0.21 [0.18-0.23]	0.25 [0.22-0.29]	0.27 [0.23-0.31]	0.30 [0.26-0.33]	<b>0.30</b> [0.27-0.32]
Activity	0.29 [0.28-0.29]	<b>0.41</b> [0.40-0.42]	<b>0.41</b> [0.40-0.42]	0.38 [0.37-0.39]	0.37 [0.36-0.37]
Average	0.25 $\pm$ 0.04	0.33 $\pm$ 0.08	<b>0.34 <math>\pm</math> 0.07</b>	<b>0.34 <math>\pm</math> 0.04</b>	0.33 $\pm$ 0.03

Table 10: **Multi-class classification comparison against CL methods.** The parameter size and reference are denoted next to their names. 95% CIs are reported in square brackets and the best value is **bolded**.

Classification - ACC ( $\uparrow$ )	Stat. Features	SimCLR (Chen et al., 2020)	BYOL (Grill et al., 2020)	TF-C (Zhang et al., 2022)	PAPAGEI-P (5M)	PAPAGEI-S (5.7M)
Operation Type	0.27 [0.24-0.32]	0.27 [0.24-0.29]	<b>0.31</b> [0.27-0.34]	0.27 [0.27-0.29]	0.30 [0.26-0.33]	0.30 [0.27-0.32]
Activity	0.37 [0.36-0.38]	<b>0.36</b> [0.35-0.37]	0.34 [0.33-0.35]	0.37 [0.36-0.38]	<b>0.38</b> [0.37-0.39]	0.37 [0.36-0.37]
Average	0.32 $\pm$ 0.05	0.31 $\pm$ 0.04	0.32 $\pm$ 0.01	0.32 $\pm$ 0.05	<b>0.34 <math>\pm</math> 0.04</b>	0.33 $\pm$ 0.03

### D.2 OTHER EVALUATION METRICS

Table 11: **Downstream comparison against pre-trained models (additional metrics: F1-score and  $R^2$ ).** The parameter size and reference are denoted next to their names. 95% CIs are reported in square brackets and the best value is **bolded**.

Classification - F1-Score ( $\uparrow$ )	REGLE (0.07M) (Yun et al., 2024)	Chronos (200M) (Ansari et al., 2024)	Moment (385M) (Goswami et al., 2024)	PAPAGEI-P (5M)	PAPAGEI-S (5.7M)
ICU Admission	0.00 [0.00-0.00]	0.20 [0.11-0.30]	0.12 [0.04-0.20]	0.12 [0.04-0.20]	<b>0.26</b> [0.18-0.33]
Mortality	0.00 [0.00-0.00]	0.14 [0.09-0.19]	0.16 [0.11-0.21]	<b>0.22</b> [0.16-0.27]	0.17 [0.13-0.22]
Smoker	0.16 [0.10-0.23]	<b>0.51</b> [0.44-0.58]	0.40 [0.33-0.47]	0.45 [0.38-0.51]	0.45 [0.37-0.50]
Pregnancy stage	0.49 [0.47-0.52]	<b>0.69</b> [0.67-0.71]	0.63 [0.60-0.65]	0.62 [0.59-0.64]	0.65 [0.62-0.67]
Hypertension	0.77 [0.70-0.84]	0.68 [0.58-0.77]	0.75 [0.66-0.84]	<b>0.84</b> [0.72-0.92]	0.78 [0.70-0.86]
Sleep Disordered Breathing	0.00 [0.00-0.00]	0.33 [0.00-0.60]	0.22 [0.00-0.47]	0.32 [0.00-0.60]	<b>0.47</b> [0.23-0.67]
Mood Disturbance	0.00 [0.00-0.00]	0.36 [0.10-0.59]	0.23 [0.00-0.47]	<b>0.37</b> [0.00-0.66]	0.32 [0.00-0.58]
Valence	0.00 [0.00-0.00]	0.10 [0.07-0.14]	0.12 [0.09-0.16]	<b>0.17</b> [0.13-0.21]	0.03 [0.01-0.04]
Arousal	0.83 [0.81-0.84]	0.82 [0.80-0.83]	0.81 [0.79-0.82]	0.81 [0.79-0.82]	<b>0.83</b> [0.81-0.84]
Average	0.25 $\pm$ 0.33	0.42 $\pm$ 0.24	0.38 $\pm$ 0.26	0.43 $\pm$ 0.25	<b>0.44 <math>\pm</math> 0.25</b>
Regression - $R^2$ ( $\uparrow$ )					
Apnea/Hypopnea Index > 3%	0.02 [0.00-0.03]	0.18 [0.08-0.26]	0.14 [0.06-0.22]	0.15 [0.05-0.24]	<b>0.29</b> [0.22-0.36]
Apnea/Hypopnea Index > 4%	0.01 [0.00-0.03]	0.16 [0.08-0.22]	0.13 [0.05-0.20]	0.12 [0.03-0.22]	<b>0.28</b> [0.20-0.34]
Gestation Age	0.04 [0.02-0.06]	<b>0.28</b> [0.24-0.31]	0.20 [0.17-0.23]	0.18 [0.14-0.22]	0.22 [0.19-0.25]
Systolic BP (VV)	-0.03 [-0.18-0.01]	-0.24 [-0.72-0.03]	0.06 [-0.25-0.28]	-0.41 [-0.77-(-0.15)]	<b>0.15</b> [-0.09-0.30]
Diastolic BP (VV)	0.01 [-0.09-0.06]	-0.29 [-0.87-(-0.01)]	0.01 [-0.25-0.14]	-0.48 [-1.02-(-0.20)]	<b>0.10</b> [-0.11-0.23]
Systolic BP (PPG-BP)	-0.07 [-0.21-0.04]	-0.13 [-0.36-0.06]	0.07 [-0.31-0.31]	<b>0.36</b> [0.16-0.49]	0.20 [0.02-0.31]
Diastolic BP (PPG-BP)	0.01 [-0.05-0.02]	-0.10 [-0.45-0.07]	-0.03 [-0.31-0.13]	<b>0.22</b> [-0.13-0.40]	0.08 [-0.07-0.17]
Average HR	0.37 [0.17-0.51]	0.02 [-0.16-0.17]	0.68 [0.45-0.80]	<b>0.79</b> [0.57-0.90]	0.78 [0.69-0.83]
HR	0.00 [0.00-0.01]	0.57 [0.56-0.59]	<b>0.63</b> [0.61-0.64]	0.52 [0.51-0.53]	0.48 [0.42-0.46]
Average	0.04 $\pm$ 0.12	0.05 $\pm$ 0.25	0.21 $\pm$ 0.24	0.16 $\pm$ 0.38	<b>0.28 <math>\pm</math> 0.20</b>

Table 12: **Downstream comparison against CL models (additional metrics: F1-score and  $R^2$ ).** The parameter size and reference are denoted next to their names. 95% CIs are reported in square brackets and the best value is **bolded**.

Classification - F1-Score ( $\uparrow$ )	Stat. Features	SimCLR	BYOL	TF-C	PAPAGEI-P (5M)	PAPAGEI-S (5.7M)
ICU Admission	<b>0.30</b> [0.18-0.40]	0.19 [0.12-0.26]	0.17 [0.11-0.22]	0.10 [0.05-0.16]	0.12 [0.04-0.20]	0.26 [0.18-0.33]
Mortality	0.03 [0.01-0.06]	0.15 [0.10-0.20]	0.13 [0.08-0.17]	0.15 [0.10-0.20]	<b>0.22</b> [0.16-0.27]	0.17 [0.13-0.22]
Smoker	0.47 [0.40-0.53]	0.43 [0.35-0.49]	<b>0.49</b> [0.42-0.56]	0.37 [0.30-0.44]	0.45 [0.38-0.51]	0.45 [0.37-0.50]
Pregnancy stage	0.43 [0.41-0.47]	0.60 [0.57-0.63]	0.60 [0.57-0.63]	0.59 [0.56-0.62]	0.62 [0.59-0.64]	<b>0.65</b> [0.62-0.67]
Hypertension	0.73 [0.58-0.85]	0.82 [0.73-0.89]	0.81 [0.73-0.88]	0.81 [0.72-0.89]	<b>0.84</b> [0.72-0.92]	0.78 [0.70-0.86]
Sleep Disordered Breathing	0.00 [0.00-0.00]	0.46 [0.21-0.64]	0.45 [0.23-0.62]	0.19 [0.00-0.36]	0.32 [0.00-0.60]	<b>0.47</b> [0.23-0.67]
Mood Disturbance	0.21 [0.00-0.47]	0.21 [0.00-0.44]	0.37 [0.00-0.67]	<b>0.56</b> [0.27-0.80]	0.37 [0.00-0.66]	0.32 [0.00-0.58]
Valence	0.04 [0.02-0.07]	0.09 [0.06-0.12]	0.01 [0.00-0.03]	0.07 [0.04-0.09]	<b>0.17</b> [0.13-0.21]	0.03 [0.01-0.04]
Arousal	0.82 [0.81-0.83]	0.81 [0.79-0.82]	<b>0.83</b> [0.81-0.84]	0.81 [0.80-0.83]	0.81 [0.79-0.82]	<b>0.83</b> [0.81-0.84]
Average	0.33 $\pm$ 0.28	0.42 $\pm$ 0.26	0.43 $\pm$ 0.27	0.40 $\pm$ 0.27	0.43 $\pm$ 0.25	<b>0.44 <math>\pm</math> 0.25</b>
<b>Regression - <math>R^2</math> (<math>\uparrow</math>)</b>						
Apnea/Hypopnea Index > 3%	-0.00 [-0.06-0.03]	0.16 [0.07-0.23]	0.16 [0.08-0.22]	0.06 [-0.00-0.13]	0.15 [0.05-0.24]	<b>0.29</b> [0.22-0.36]
Apnea/Hypopnea Index > 4%	-0.01 [-0.07-0.03]	0.13 [0.06-0.21]	0.13 [0.05-0.19]	0.13 [-0.06-0.26]	0.12 [0.03-0.22]	<b>0.28</b> [0.20-0.34]
Gestation Age	0.07 [0.04-0.10]	0.19 [0.15-0.21]	0.19 [0.15-0.22]	0.18 [0.15-0.21]	0.18 [0.14-0.22]	<b>0.22</b> [0.19-0.25]
Systolic BP (VV)	-0.10 [-0.51-0.10]	-0.05 [-0.44-0.21]	-0.03 [-0.37-0.18]	-0.05 [-0.36-0.12]	-0.41 [-0.77-(-0.15)]	<b>0.15</b> [-0.09-0.30]
Diastolic BP (VV)	-0.15 [-0.31-0.11]	-0.14 [-0.29-0.08]	-0.01 [-0.40-0.20]	-0.09 [-0.45-0.16]	-0.48 [-1.02-(-0.20)]	<b>0.10</b> [-0.11-0.23]
Systolic BP (PPG-BP)	0.12 [-0.04-0.21]	0.09 [-0.20-0.31]	0.10 [-0.16-0.30]	0.13 [-0.06-0.26]	<b>0.36</b> [0.16-0.49]	0.20 [0.02-0.31]
Diastolic BP (PPG-BP)	0.01 [-0.18-0.14]	0.00 [-0.20-0.18]	0.05 [-0.11-0.17]	0.02 [-0.15-0.12]	<b>0.22</b> [-0.13-0.40]	0.08 [-0.07-0.17]
Average HR	0.15 [-0.10-0.33]	0.74 [0.64-0.80]	0.65 [0.50-0.77]	<b>0.82</b> [0.73-0.88]	0.79 [0.57-0.90]	0.78 [0.69-0.83]
HR	0.34 [0.32-0.36]	0.45 [0.44-0.47]	0.36 [0.35-0.37]	<b>0.54</b> [0.53-0.55]	0.52 [0.51-0.53]	0.48 [0.42-0.46]
Average	0.05 $\pm$ 0.14	0.17 $\pm$ 0.25	0.18 $\pm$ 0.20	0.19 $\pm$ 0.28	0.16 $\pm$ 0.38	<b>0.28 <math>\pm</math> 0.20</b>

Table 13: **Scaling: Downstream comparison for different PAPAGEI-S models.** 95% CIs are reported in square brackets and the best value is **bolded**.

Classification - AUROC ( $\uparrow$ )	PAPAGEI-S-5M	PAPAGEI-S-35M	PAPAGEI-S-139M
ICU Admission	<b>0.79</b> [0.75-0.82]	0.72 [0.68-0.75]	0.77 [0.73-0.80]
Mortality	<b>0.67</b> [0.63-0.70]	0.66 [0.63-0.70]	0.66 [0.63-0.69]
Smoker	<b>0.61</b> [0.56-0.66]	0.58 [0.52-0.64]	0.59 [0.54-0.65]
Pregnancy stage	<b>0.78</b> [0.75-0.80]	0.77 [0.75-0.79]	0.76 [0.74-0.78]
Hypertension	<b>0.77</b> [0.68-0.87]	0.75 [0.64-0.85]	<b>0.77</b> [0.65-0.87]
Sleep Disordered Breathing	<b>0.70</b> [0.57-0.84]	0.59 [0.44-0.74]	0.62 [0.46-0.78]
Mood Disturbance	<b>0.56</b> [0.33-0.77]	0.53 [0.30-0.73]	0.54 [0.29-0.78]
Valence	<b>0.56</b> [0.54-0.59]	0.53 [0.50-0.56]	0.54 [0.51-0.56]
Arousal	<b>0.55</b> [0.52-0.57]	0.52 [0.49-0.55]	<b>0.55</b> [0.52-0.58]
Average	<b>0.67 <math>\pm</math> 0.09</b>	0.63 $\pm$ 0.09	0.63 $\pm$ 0.10
<b>Regression - MAE (<math>\downarrow</math>)</b>			
Apnea/Hypopnea Index > 3%	12.97 [11.87-14.05]	13.07 [11.92-14.25]	<b>12.86</b> [11.79-13.94]
Apnea/Hypopnea Index > 4%	<b>10.56</b> [9.59-11.62]	10.79 [9.85-11.83]	10.65 [9.62-11.68]
Gestation Age	<b>6.05</b> [5.91-6.17]	6.10 [5.94-6.24]	6.17 [6.02-6.30]
Systolic BP (VV)	<b>14.65</b> [12.50-16.78]	15.10 [13.10-17.21]	14.95 [12.87-17.01]
Diastolic BP (VV)	<b>8.29</b> [6.61-10.22]	9.20 [6.93-11.12]	8.95 [6.72-10.95]
Systolic BP (PPG-BP)	<b>14.39</b> [12.53-16.45]	16.70 [14.25-19.38]	16.20 [13.73-18.85]
Diastolic BP (PPG-BP)	<b>8.71</b> [7.18-10.01]	9.48 [8.24-10.90]	9.32 [7.90-10.69]
Average HR	<b>4.00</b> [3.34-4.67]	4.76 [3.94-5.86]	4.71 [3.86-5.60]
HR	<b>11.53</b> [11.40-11.66]	12.86 [12.73-12.99]	12.20 [12.07-12.34]
Average	<b>10.12 <math>\pm</math> 3.47</b>	10.89 $\pm$ 3.73	10.76 $\pm$ 3.57

## E EFFECT OF SKIN TONE

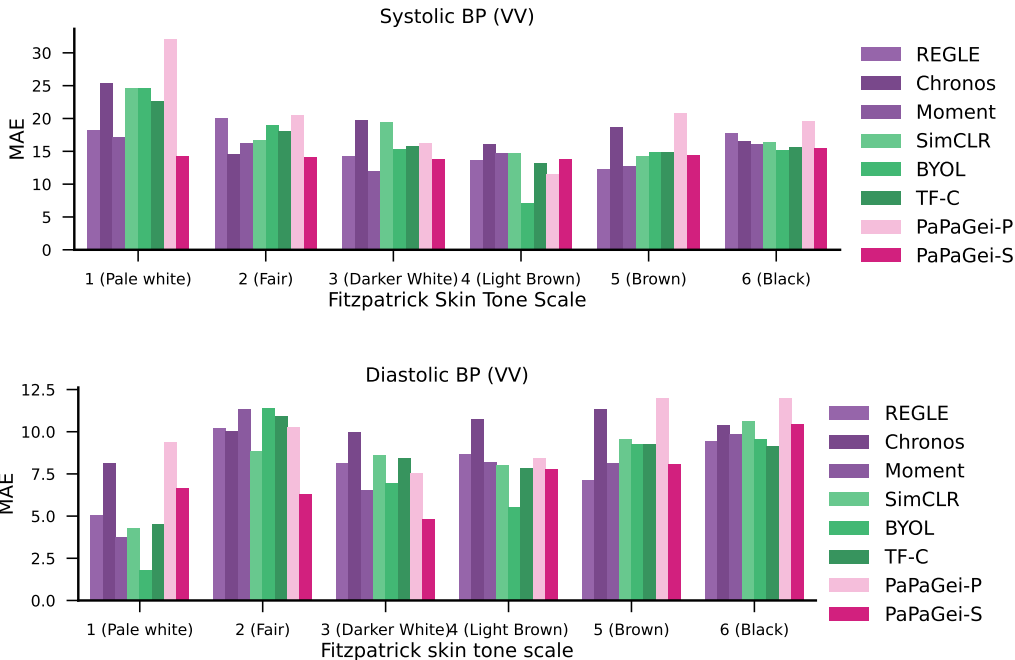


Figure 22: Detailed skin tone analysis for Blood Pressure estimation (VV dataset).

## F EXTENDED RELATED WORK

Self-supervised learning (SSL) is the most prominent paradigm for learning general representations from large unlabeled datasets, including methods like SimCLR (Chen et al., 2020), BYOL (Grill et al., 2020), and masked autoencoders (MAE) (He et al., 2022). Timeseries-specific objectives like TNC and TF-C have also shown promise (Tonekaboni et al., 2021; Zhang et al., 2022). SSL has gained traction in the domain of physiological signal analysis, with applications to health records (Chen et al., 2021; Yèche et al., 2021), fitness and personalization (Spathis et al., 2021), as well as brain (Cheng et al., 2020) and heart signals (Kiyasseh et al., 2021; Sarkar & Etemad, 2020).

However, despite the popularity of SSL, there are no widely used pre-trained models for PPG data. A recent study (Abbaspourazad et al., 2023) demonstrated that embeddings derived from ECG and PPG signals can generalize across multiple health outcomes using proprietary large-scale data. While this work showcased the potential of foundation models for physiological signals, it was based on a single dataset and device (Apple Watch) while the models were not released, limiting its practical use in the research community. Similarly, REGLE’s work (Yun et al., 2024) on the UK Biobank dataset showed that embedding PPG signals can improve genetic discovery and risk prediction outcomes. Although parts of that model and pipeline are public, the dataset is not openly accessible, and the primary goal was not to create a foundation model for PPG but rather to focus on genetics. Another work on the same data showed that PPG embeddings are promising for cardiovascular risk prediction (Weng et al., 2024). SiamQuality (Ding et al., 2024) also trained an unreleased model on 36 million PPG signals using proprietary data. Importantly, most of these works pre-trained on a single-device dataset and did not explore out-of-domain datasets or conduct transfer learning experiments, which are crucial for assessing the true generalizability of foundation models. These studies highlight the potential of PPG-based foundation models but also underscore the need for openly available, pre-trained models that can be widely used and adapted by the research community.

---

On the other hand, generic time series foundation models have begun to gain popularity, mirroring the trend seen in Large Language Models (LLMs). These models are pre-trained on massive corpora of diverse time series data, aiming to learn universal representations that can be applied across various domains. For instance, Chronos (Ansari et al., 2024) was trained on an impressive 84 billion observations (analogous to tokens in NLP) from 28 distinct datasets. However, it’s notable that this diverse collection does not include physiological data. Similarly, Moment (Goswami et al., 2024) was trained on billions of observations from a wide-ranging dataset that includes weather, traffic, energy, and other domains. While Moment does incorporate a small amount of ECG data, it comprises only a tiny percentage of the overall data pool.

In contrast to these generic approaches, our work takes a domain-specific focus. We curate a large pre-training and evaluation benchmark dedicated exclusively to PPG data. While knowledge gained from generic time series foundation models may transfer to domain-specific tasks like PPG, we expect the performance to be limited compared to a model trained specifically on PPG data. Furthermore, foundation models for ECG (McKeen et al., 2024; Song et al., 2024) or EEG (Yuan et al., 2024b) have shown promise but transferring from one domain-specific model (e.g., ECG) to another (PPG) is likely to be even more challenging, as the underlying signal characteristics can be quite different. Building on the increasing interest in modality-specific foundation models, our specialized approach allows us to capture nuances and complexities specific to PPG signals.

An increasingly popular approach involves feeding timeseries data and prompts directly to Large Language Models (LLMs) (Gruver et al., 2024). However, despite promising results, LLMs struggle with high-dimensional signals due to their text-based processing (Spathis & Kawsar, 2024). A modality-specific encoder like PAPAGEI addresses this limitation by providing representations of raw signals (Belyaeva et al., 2023), which can be combined with text and fed into more powerful multimodal foundation models, such as AnyMAL (Moon et al., 2023). This approach offers several advantages: computational efficiency through a fixed LLM, flexibility due to the modular design of encoder, adapter, and LLM components, and interoperability with other high-performing models (e.g., a state-of-the-art IMU encoder (Yuan et al., 2024a)). Crucially, this encoder-LLM approach does not require paired data with other modalities to train a single multimodal model. However, it may introduce complexity by limiting end-to-end gradient propagation and reduce interpretability in encoder-LLM communication compared to natural language prompts. Despite these trade-offs, PAPAGEI serves dual purposes: as a generic feature extractor for various PPG signals and applications, and as a modality encoder in next-generation frontier models. This versatility positions it as a valuable tool for advancing multimodal sensory AI systems.

## G EXTENDED DISCUSSION

Our results show that PAPAGEI outperforms baselines in at least 14 out of 20 tasks, with average classification and regression improvements of 4.7%-6.3% and 2.9%-4.9%, respectively (Section 5.1). PAPAGEI-S performed best for cardiovascular parameters like BP, Hypertension, and Avg. HR, which are closely linked to components such as sVRI and IPA (Liang et al., 2018b). Additionally, PAPAGEI-P surpassed pre-trained baselines like Moment and is well-suited for tasks such as Smoking and Arousal.

By ablating different components of PAPAGEI-S (Section 5.2), we found that the full model performs best, with sVRI contributing the most. Adding IPA or SQI separately did not improve performance, suggesting that (a) IPA and SQI positively transfer in a multi-task setup, and (b) our design choice to include both to compensate for situations where IPA cannot be computed is effective (Section 3.2). While combining PAPAGEI-P and PAPAGEI-S may seem intuitive, constraining positive pairs on both sVRI and participants leads to too many unique labels with limited samples. In our scalability analysis, we observed that the smallest model (5M parameters) outperformed others, aligning with other studies using CNNs with 3.3M parameters for biosignals (Abbaspourazad et al., 2023), likely due to the size of PPG datasets. Larger models like Chronos or Moment are impractical for wearables due to their size and privacy concerns with cloud-based inference for health data. Additionally, PAPAGEI-S is more data-efficient for linear probing, showing greater performance gains with increased data availability, making it a promising backbone for small studies in future research.

Our studies in Section 5.3 reveal that PAPAGEI-S embeddings are more dispersed across participants, enhancing performance, while regression predictions more accurately reflect the true distribu-

---

tion. We attribute this to our positive pair selection, which chooses positive pairs across individuals based on sVRI. Moreover, our skin tone analysis shows that the method performs better on lighter skin tones, likely due to the model being trained predominantly on such data. For darker skin tones, performance was similar across models for diastolic BP, with REGLE and BYOL performing best, highlighting the need for future work creating more robust models for diverse skin tones.